THE SPRAY CONTRIBUTION TO NET EVAPORATION FROM THE SEA: A REVIEW OF RECENT PROGRESS

EDGAR L ANDREAS,[1] JAMES B. EDSON,[2] EDWARD C. MONAHAN,[3], MATHIEU P. ROUAULT,[4] and STUART D. SMITH[5]

[1]*U.S. Army Cold Regions Research and Engineering Laboratory, Hanover, New Hampshire 03755, U.S.A.;* [2]*Department of Applied Ocean Physics, Woods Hole Oceanographic Institution, Woods Hole, Massachusetts 02543, U.S.A.;* [3]*Marine Sciences Institute, University of Connecticut at Avery Point, Groton, Connecticut 06340, U.S.A.;* [4]*Department of Oceanography, University of Cape Town, 7700 Rondebosch, Republic of South Africa;* [5]*Department of Fisheries and Oceans, Bedford Institute of Oceanography, Dartmouth, Nova Scotia B2Y 4A2, Canada*

(Received in final form 18 May, 1994)

Abstract. The part that sea spray plays in the air-sea transfer of heat and moisture has been a controversial question for the last two decades. With general circulation models (GCMs) suggesting that perturbations in the Earth's surface heat budget of only a few W m^{-2} can initiate major climatic variations, it is crucial that we identify and quantify all the terms in that heat budget. Thus, here we review recent work on how sea spray contributes to the sea surface heat and moisture budgets. In the presence of spray, the near-surface atmosphere is characterized by a droplet evaporation layer (DEL) with a height that scales with the significant-wave amplitude. The majority of spray transfer processes occur within this layer. As a result, the DEL is cooler and more moist than the atmospheric surface layer would be under identical conditions but without the spray. Also, because the spray in the DEL provides elevated sources and sinks for heat and moisture, the vertical heat fluxes are no longer constant with height. We use Eulerian and Lagrangian models and a simple analytical model to study the processes important in spray droplet dispersion and evaporation within this DEL. These models all point to the conclusion that, in high winds (above about 15 m/s), sea spray begins to contribute significantly to the air-sea fluxes of heat and moisture. For example, we estimate that, in a 20-m/s wind, with an air temperature of 20°C, a sea surface temperature of 22°C, and a relative humidity of 80%, the latent and sensible heat fluxes resulting from the spray alone will have magnitudes of order 150 and 15 W/m^2, respectively, in the DEL. Finally, we speculate on what fraction of these fluxes rise out of the DEL and, thus, become available to the entire marine boundary layer.

1. Introduction

Pioneers such as Bortkovskii (1973, 1983, 1987), Borisenkov (1974), Wu (1974), and Ling (Ling and Kao, 1976; Ling *et al.*, 1978, 1980), who tried to estimate the contribution of sea spray droplets to evaporation from the sea surface, faced many uncertainties. For example, they did not have reliable estimates of the flux of spray droplets up from the ocean surface and did not have a clear understanding of how evaporation from spray droplets modifies the temperature and humidity profiles in the lower marine boundary layer.

Although we have learned much about these processes in the last decade, many uncertainties remain. The field is, therefore, still rife with controversy because experimental work is difficult, the processes are complex and interactive, and theories of sea spray generation and heat and moisture transfer by spray are still rudimentary. The recent exchanges in the literature between Monahan and Woolf

Boundary-Layer Meteorology **72:** 3–52, 1995.

(1989) and Wu (1988b, 1989b), between Woolf (1990) and Wu (1989a, 1990c), between Wu (1990a) and Blanchard and Syzdek (1988, 1990), between de Leeuw (1990a) and Wu (1990d), between Andreas (1994a) and Hasse (1992, 1994), and between Katsaros and de Leeuw (1994) and Andreas (1992, 1994b) are evidence that this field is vibrant and still evolving. Contrary to Ling's (1993) claim, the "mystery" is far from solved. Thus, to identify the work yet to be done, we here summarize our current understanding of the role that spray plays in evaporation from the sea.

2. Sea Spray Production Mechanisms

A key to more accurate estimates of the magnitude of the wind-dependent sea spray generation function lies in identifying the physical mechanisms that produce spray droplets of various sizes. For example, wave-breaking causes entrainment of air. The resulting bubbles in the subsurface plume or cloud (Thorpe, 1982, 1983; Thorpe and Hall, 1983; Monahan and Lu, 1990) will, upon rising into a whitecap, produce at least some of these droplets (Jacobs, 1937; Woodcock, 1972).

Thanks largely to Blanchard's (1963) seminal work, it is clear that two distinct types of droplets form when the bubbles in whitecaps burst. When the upper, protruding surface of a bubble rising to the air-sea interface thins sufficiently (as it typically does within a second of the bubble's arrival at the sea surface), it shatters (Figure 1), producing anywhere from a few to a few hundred film droplets. Although Resch (1986) and Resch and Afeti (1991) showed that such droplets can have initial radii greater than 20 μm, these film droplets are typically much smaller and are now recognized as the predominant component of the droplet flux spectrum for radii less than 3 μm (Woolf *et al.*, 1987). In earlier studies, Woodcock (1972) concluded that film droplets predominate at radii below 0.2-0.5 μm, while Cipriano and Blanchard (1981) deduced that these droplets are the primary components of the surface droplet flux at radii less than 7.5 μm.

Jet droplets are the second category of bubble-generated sea spray. These droplets, one to six in number (Blanchard, 1983; Resch and Afeti, 1991; Spiel, 1992), are pinched off the end of the microscopic column of water that rises out of the center of the collapsing cavity left after the bubble cap ruptures (see Figure 1 and Kientzler *et al.*, 1954). This column, or Rayleigh jet, results from the rebound, or overshoot, of the sea surface caused by its surface tension. Jet droplets typically dominate the spray droplet flux spectrum in the 3–20 μm radius range.

In contrast to these two kinds of indirectly produced droplets, wave breaking can directly produce other droplets without the mediation of bubbles (Figure 1). Spume droplets result from the mechanical tearing of the sharpened wave crests by the wind (Monahan *et al.*, 1983a, 1986; Monahan, 1986). Splash droplets are a consequence of the vigorous spilling, or curling over, of the crests of breaking

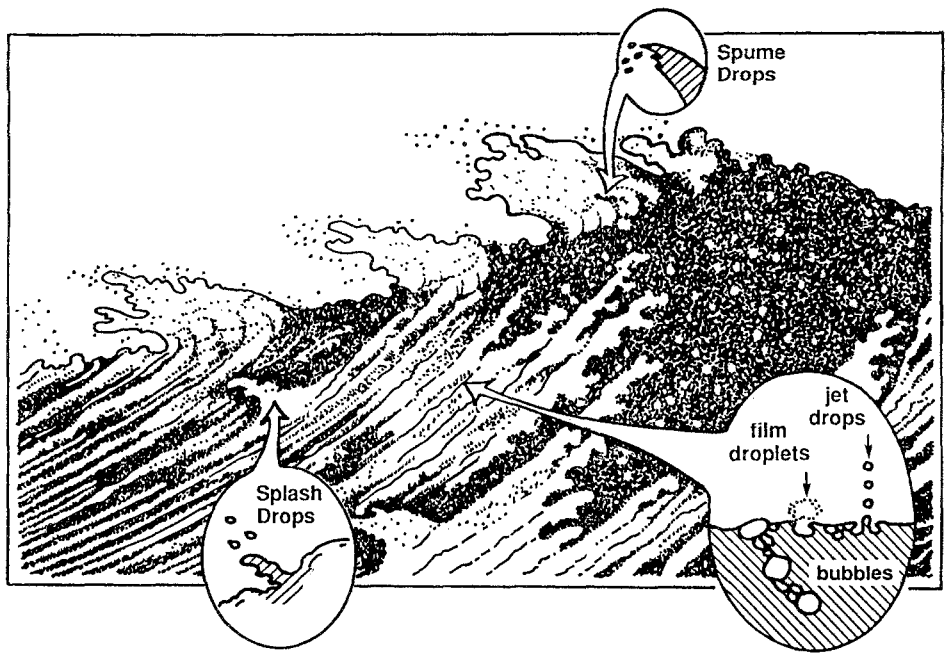

Fig. 1. Origins of the various kinds of sea spray droplets. Splash droplets arise where wave crests spill, i.e., at the sites of Stage-A whitecaps. Most film and jet droplets are produced by Stage-B whitecaps, i.e., where bubbles rise and burst. Spume droplets are torn directly from the crests of steep waves. The general form of this wave, the spume droplet clouds, etc., are based on an illustration by Hokusai (c. 1833).

waves. On formation, spume and splash droplets typically have radii larger than 20 μm.

The common belief is that spume cannot form until the 10-m wind speed is at least 9 m/s. Wu (1993) recently argued, however, that the near-surface droplet concentrations that Wu *et al.* (1984) measured showed evidence of spume production in a 10-m wind of only 7.5 m/s. Thus, it is time to equivocate: this 9-m/s threshold for spume production, which seems to have been derived, though inappropriately, from Ross and Cardone (1974; Monahan and O'Muircheartaigh, 1980), is at best a rule of thumb. We prefer to say that the wind speed threshold for spume production is 7–11 m/s (Monahan *et al.*, 1983b; Wu, 1993); the actual threshold depends on such things as water temperature, the wave field, and the

turbulence intensity in the near-surface air. This 7–11 m/s range corresponds roughly to Beaufort Force 5, which includes the "chance of some spray" (meaning spume here) as one of its defining characteristics (Pierson, 1990).

The bubble-mediated components of the sea surface spray flux are directly related to the rate at which air is entrained into the oceanic surface layer. With the approximation that the concentration of bubbles in a subsurface plume diminishes exponentially with depth (Thorpe, 1982; Monahan, 1993), this rate is simply proportional to the rate of oceanic whitecap formation. In turn, when wind and sea are in dynamic equilibrium, the rate of whitecap area formation is equal to the rate of whitecap area decay. Because the area of each whitecap decreases exponentially with time, the rate of whitecap area formation, or decay, is directly proportional to the instantaneous fraction of the sea surface covered by whitecaps (Monahan, 1971). Models for the bubble-mediated sea spray generation function, $\mathrm{d}F_b/\mathrm{d}r_0$, where r_0 refers to the initial radii of the spray droplets, have been developed in which this generation function is explicitly proportional to W_B, the fraction of the sea surface covered at any instant by decaying (Stage-B) whitecaps (Monahan *et al.*, 1982, 1986). That is,

$$\frac{\mathrm{d}F_b}{\mathrm{d}r_0} \propto \dot{W}_B \propto W_B, \tag{1}$$

where the over-dot indicates a time derivative.

Various investigators have attempted to describe whitecap coverage in terms of wind speed and other meteorological parameters (e.g., Blanchard, 1963; Monahan, 1971; Monahan and O'Muircheartaigh, 1980, 1986; Wu, 1979a, 1988b). The rate of whitecap area formation, $\dot{W}_B$, should be related to the rate at which the wind supplies energy to the sea surface, $\dot{E}$. In turn, this energy flux is related to the product of the surface stress, $\tau = \rho_a u_*^2$, and the speed of the surface drift current, u_s (Wu, 1979a);

$$\dot{W}_B \propto \dot{E} \propto \tau u_s, \tag{2}$$

where ρ_a is air density, and u_* is friction velocity. Lastly, because u_s is proportional to u_*, Equations (1) and (2) predict that the wind dependence for the production of bubble-derived spray droplets should be

$$\frac{\mathrm{d}F_b}{\mathrm{d}r_0} \propto u_*^3. \tag{3}$$

Comparable expressions have been proposed that give the production rate of bubble-derived spray droplets in terms of the wind speed at 10 m (Monahan *et al.*, 1983a, 1986; Miller and Fairall, 1988; Exton *et al.*, 1985).

The wind dependence of splash droplet production should follow the wind dependence of film and jet droplet production. Splash droplet production and

the rate of injection into the sea of the bubbles that give rise to film and jet droplets are both essentially proportional to the wave breaking, which in turn is proportional to the fraction of the sea surface covered by decaying whitecaps.

The process that forms spume droplets, on the other hand, is not as clearly associated with whitecap coverage. To form spume, the wind must supply energy to create new surfaces: it must change the free energy (or Helmholtz free energy; Iribarne and Godson, 1981, p. 40) of the system. According to Dufour and Defay (1963, p. 154 ff.), when a single droplet is formed, the change in system free energy, ΔF, must be

$$\Delta F = -V(p_{\text{in}} - p_{\text{out}}) + \sigma\Omega, \tag{4}$$

where V is the droplet's volume, Ω is its surface area, and σ is the surface tension of sea water. Laplace's equation (Dufour and Defay, 1963, p. 4) gives the difference in pressure between the inside (p_{in}) and the outside (p_{out}) of the droplet,

$$p_{\text{in}} - p_{\text{out}} = \frac{2\sigma}{r_0}, \tag{5}$$

where r_0 is, again, the initial radius of the droplet. Substituting this into Equation (4) gives the free energy required to form a single droplet,

$$\Delta F = \frac{1}{3}\sigma\Omega. \tag{6}$$

From Equation (6), we see that when spume droplets form continually, the time rate of change of free energy of the system per unit of sea surface area, $\Delta\dot{\text{F}}$, must relate to the rate of total droplet surface area formed, $\dot{\Omega}_T$. That is,

$$\Delta\dot{\text{F}} = \frac{1}{3}\sigma\dot{\Omega}_T, \tag{7}$$

where

$$\dot{\Omega}_T = 4\pi \int_0^\infty r_0^2 \frac{\mathrm{d}F_s}{\mathrm{d}r_0}\mathrm{d}r_0. \tag{8}$$

Here, $\mathrm{d}F_s/\mathrm{d}r_0$ is the generation function for spume droplets of initial radius r_0.

Notice that $\Delta\dot{\text{F}}$ has units of W m^{-2} – it represents an energy flux. Thus, as with whitecaps, we hypothesize that

$$\dot{\Omega}_T \propto \Delta\dot{\text{F}} \propto \tau U. \tag{9}$$

That is, the generation rate for the total surface area of spume droplets must be proportional to the energy flux from the wind.

In Equation (9), the velocity scale U should be appropriate at the wave crests, where the spume originates. Modelling this height as the significant wave amplitude $A_{1/3}$ – the mean height above sea level of the highest one-third of the waves – we write

$$U = \frac{u_*}{\kappa} \ln\left(\frac{A_{1/3}}{z_0}\right), \tag{10}$$

where κ is von Kármán's constant. To predict $A_{1/3}$, we use (Kinsman, 1965, p. 391; Wilson, 1965; Earle, 1979)

$$A_{1/3} = 0.015 U_{10}^2, \tag{11}$$

where $A_{1/3}$ is in m when the wind speed at a height of 10 m, U_{10}, is in m s^{-1}. For z_0 in Equation (10), we use Charnock's (1955) relation,

$$z_0 = \alpha \frac{u_*^2}{g}, \tag{12}$$

where g is the acceleration of gravity, $\alpha = 0.0185$ (Wu, 1988a) is the Charnock constant, and the units throughout Equation (12) are m and sec.

Thus, finally combining Equations (10)–(12) in Equation (9), we predict

$$\dot{\Omega}_T \propto u_*^3 \ln\left(\frac{0.015 g}{\alpha C_{D10}}\right), \tag{13}$$

where $C_{D10} = (u_*/U_{10})^2$ is the 10-m drag coefficient. Because, over the ocean, C_{D10} increases with wind speed (e.g., Smith *et al.*, 1992), our prediction for spume is that $\dot{\Omega}_T$ should increase somewhat slower than u_*^3. To our knowledge, this is the first formal prediction for how spume production depends on the wind.

3. Sea Spray Generation Function

To evaluate when or whether sea spray droplets contribute to the air-sea fluxes of heat and moisture, we must estimate the rate at which droplets of any given size are produced. That is, we must estimate the so-called sea spray generation function, which means trying to quantify the spray droplet production mechanism.

Before considering the spray generation function, however, we must review the microphysics of spray droplets. How rapidly does an individual spray droplet that started with radius r_0 exchange moisture (or latent heat) with its environment, given some ambient conditions? In other words, how rapidly does a droplet's radius change? Similarly, how rapidly does that droplet exchange sensible heat – i.e., change temperature? Finally, how do these rates compare with the droplet's atmospheric residence time – the time between its formation and its return to the sea surface? These rates, which are functions of r_0, determine what size range we need to consider in formulating the sea spray generation function relevant to our problem.

3.1. Spray Droplet Microphysics

Pruppacher and Klett (1978) provided a good introduction into the microphysics of aqueous solution droplets. Andreas (1989, 1990) applied their equations specifically to sea spray droplets to determine the rates at which a spray droplet with initial radius r_0 exchanges sensible and latent heat with its environment. He showed that the droplet temperature $T(t)$ as a function of time t after formation approximately follows an exponential relation;

$$\frac{T(t) - T_{eq}}{T_w - T_{eq}} = \exp(-t/\tau_T). \tag{14}$$

Here, T_w is the initial droplet temperature – assumed to be the same as the sea surface temperature – and T_{eq} is the equilibrium temperature the droplet would reach in air of temperature T_a and relative humidity RH if given enough time. The time scale τ_T in Equation (14) characterizes the rate of temperature change or, alternatively, the sensible heat flux attributable to the droplet. Clearly, in time τ_T, the droplet undergoes 63% of its potential temperature change.

Andreas (1989) proposed a relation similar to Equation (14) to model the instantaneous droplet radius $r(t)$ for $t \leq \tau_r$;

$$\frac{r(t) - r_{eq}}{r_0 - r_{eq}} = \exp(-t/\tau_r), \tag{15}$$

where r_{eq} is the radius the droplet would have if given time to reach moisture equilibrium with ambient conditions. The droplet is assumed to start with an initial salinity S that is the same as in the surface sea water. For $t > \tau_r$, Equation (15) is no longer accurate, and the full microphysical equations must be used to predict the size evolution (Andreas, 1989, 1990).

In Equation (15), τ_r characterizes the rate of radius evolution or, alternatively, the flux of moisture or latent heat from the droplet. In time τ_r, a droplet has experienced 63% of its potential radius change; or, if the relative humidity is 95% or less, it will have lost at least two-thirds of the water it must lose to reach equilibrium (Andreas, 1990).

Figure 2 shows typical τ_T and τ_r values. Andreas (1989, 1990) presented similar plots for other ambient conditions. The startling fact obvious from the curves for τ_T and τ_r in Figure 2 is the large difference in their magnitudes. Virtually all spray droplets reach thermal equilibrium within 1 s. Although the smallest spray droplets reach moisture equilibrium within 1 s, the largest droplets require an hour or more to reach moisture equilibrium. In effect, the transfers of sensible and latent heat from a spray droplet are decoupled; the droplet will have exchanged all of its sensible heat long before it begins transferring latent heat. Consequently, the ambient humidity has negligible impact on a droplet's thermal evolution. Similarly, since the thermal exchange is complete before moisture

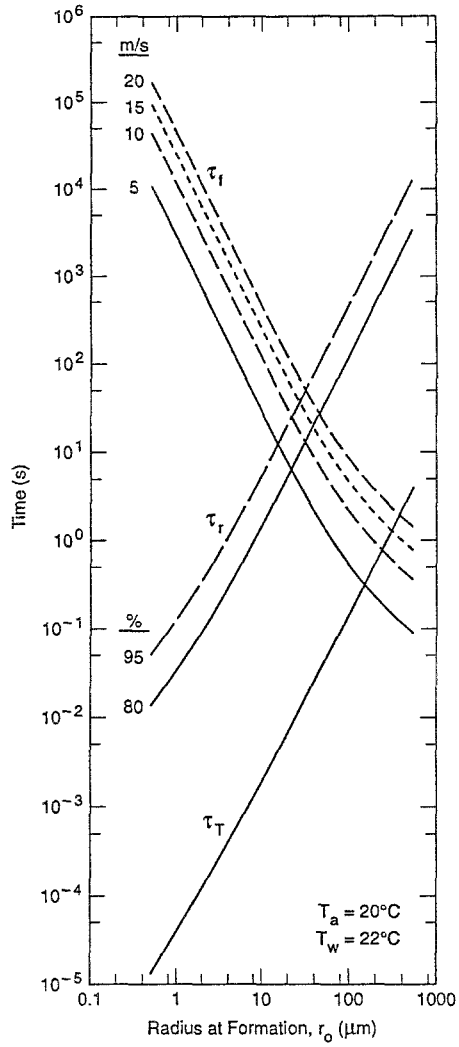

Fig. 2. The time scales τ_T, τ_r, and τ_f as functions of the initial spray droplet radius, r_0. Ambient conditions are T_a = 20°C, T_w = 22°C, salinity S of 34‰, and an atmospheric pressure P of 1000 hPa. The relative humidity, RH, is 80% and 95%, and the 10-m wind speed, U_{10}, is 5, 10, 15, and 20 m/s, as labeled.

exchange even begins, T_w can have no effect on the moisture exchange; a droplet is at T_{eq} by the time the moisture exchange begins.

The ambient air temperature, T_a, does affect both τ_T and τ_r, however. As T_a increases from −20 to 20°C, τ_T decreases by a factor of about two because some of the constants in the thermal evolution equation are temperature dependent (Andreas, 1989). For the same 40°C temperature increase, τ_r, on the other hand, decreases by more than an order of magnitude, primarily because the saturation vapor pressure is such a strong function of temperature. Warm droplets simply

exchange moisture with their surroundings more rapidly than cool droplets. Other things being equal, we thus expect spray contributions to air-sea vapor exchange to be greatest where the air is warmest.

To place any significance on the τ_T and τ_r values, we must compare them with a time scale that parameterizes a droplet's atmospheric residence time. A time scale based on the terminal fall speed, $w_s(r_0)$, is appropriate. Andreas (1989; or Wu, 1979b) gave equations for calculating w_s; these yield the Stokes terminal fall speed modified for the large Reynolds numbers that characterize the larger droplets (Batchelor, 1970, p. 234; Friedlander, 1977, p. 105).

Next, we must combine w_s with a length scale. The significant wave amplitude $A_{1/3}$ is a physical scale in this problem (Andreas, 1992; Iida *et al.*, 1992). Thus, the time characterizing the atmospheric residence of a spray droplet,

$$\tau_f = \frac{A_{1/3}}{w_s(r_0)}, \tag{16}$$

parameterizes the time required for a droplet to fall back to the sea surface from a height of $A_{1/3}$ in still air.

The use of $A_{1/3}$ as the length scale in (16) requires some justification. After all, the maximum ejection height for jet droplets is only 18 cm (Blanchard and Woodcock, 1957; Blanchard, 1963; Wu, 1979b). But turbulence in the wind field must carry the small bubble-derived droplets higher. Our modelling in the next section suggests this, and de Leeuw's (1986a, 1986b, 1987) results confirm it. The droplet concentration profiles that he measured over the open ocean show very small gradients over heights from 10–20 cm to well above 10 m for droplets with radii up to at least 40 μm. De Leeuw (1987), in fact, concluded that "the scale height for particle concentrations is 1–2 times the wave height". Also, as we shall show more clearly later, spume droplets – which are torn off the wave crests and, thus, originate roughly $A_{1/3}$ above the sea surface (Bortkovskii, 1987, p. 46; de Leeuw, 1990b; Wu, 1990b) – contribute most to the spray heat and moisture fluxes. Consequently, $A_{1/3}$ is a more appropriate length scale than one that represents droplet ejection height.

The time scale τ_f also indirectly parameterizes turbulence effects. $A_{1/3}$ increases with the square of the wind speed. This is basically the same behavior that the turbulent kinetic energy has in the atmospheric surface layer. A rising wave field is, therefore, associated with higher turbulence levels in the atmospheric boundary layer, with more efficient suspension of spray droplets, and, thus, with longer residence times. Consequently, τ_f – with $A_{1/3}$ as the length scale – not only models the location of the spume production but also seems to account, at least intuitively, for how turbulence enhances a droplet's residence time.

Figure 2 compares τ_f values with the microphysical scales τ_T and τ_r. For the smallest spray droplets, τ_f is orders of magnitude larger than both τ_T and τ_r; once created, these droplets remain suspended indefinitely and, thus, have ample time to exchange sensible and latent heat with the air. For the largest droplets,

τ_f is smaller than both τ_T and τ_r. These droplets, therefore, will likely fall back into the sea before participating fully in the exchanges of sensible and latent heat. The $\tau_f - \tau_T$ crossover occurs at radii from 100 to 400 μm, depending on the wind speed. Smaller droplets exchange most of their sensible heat before returning to the sea; larger droplets do not. Remember, droplets with r_0 greater than 20 μm are predominately spume droplets (Monahan *et al.*, 1983b, 1986). The $\tau_f - \tau_r$ crossover occurs at radii between 10 and 50 μm. Thus, the smallest droplets participate fully in the exchange of latent heat, but the largest droplets exchange almost none before falling back into the sea. Some of the droplets in this crossover region are jet droplets, but a large percentage will be spume droplets.

Figure 2 and our discussion here thus demonstrate that spume droplets are potentially important vehicles for carrying sensible and latent heat across the air-sea interface. Because of the rapidity of the sensible heat transfer especially, spume may play a pivotal role in enhancing air-sea sensible heat exchange. A useful sea spray generation function must, therefore, not only model the bubble-produced film and jet droplets but also estimate spume production. Droplet radii of concern range from tenths of micrometers to 500 μm, where Figure 2 shows that droplet residence times are too low for even the sensible heat transfer from spray droplets to be a factor in air-sea exchange.

3.2. A SAMPLING OF SPRAY GENERATION FUNCTIONS

Monahan *et al.* (1983a, 1986) were the first to present a spray generation function that explicitly predicted the production rates of both bubble-derived film and jet droplets and the mechanically produced spume droplets. Their term predicting the spray production by bursting bubbles has proved quite useful (e.g., Burk, 1984; Stramska, 1987), but their spume-production term predicts far too many spume droplets (M. H. Smith *et al.*, 1990, 1993; Andreas, 1992). Andreas (1990) and Smith *et al.* (1993) showed plots of their spray generation function.

Woolf *et al.* (1988) updated the bubble-derived term in the Monahan model with whitecap simulation tank data collected after Monahan *et al.* (1986) published their work. Because that conference paper by Woolf *et al.* is not widely available, we repeat its prediction equations here. From their simulation tank measurements, Woolf *et al.* modelled the total spray droplet number flux from a single whitecap, $\mathrm{d}E/\mathrm{d}r_{80}$, as

$$\frac{\mathrm{d}E}{\mathrm{d}r_{80}} = \exp[16.1 - 3.43(\log r_{80}) - 2.49(\log r_{80})^2 + 1.21(\log r_{80})^3]. \qquad (17)$$

Here, $\mathrm{d}E/\mathrm{d}r_{80}$ is the number of droplets produced during the decay of a whitecap per m^2 of whitecapped surface per μm increment in the droplet radius r_{80}, where r_{80} is the droplet radius in μm at a reference relative humidity of 80% (Fairall

et al., 1983). From Equation (17), Woolf *et al.* then estimated the actual oceanic number flux of bubble-derived spray droplets as (e.g., Monahan *et al.*, 1982)

$$\frac{\mathrm{d}F_W}{\mathrm{d}r_{80}} = \frac{W_B(U_{10})}{\tau_d}\frac{\mathrm{d}E}{\mathrm{d}r_{80}}, \tag{18}$$

where $\tau_d = 3.53$ s is the typical decay time of a whitecap (Monahan *et al.*, 1982, 1986), and $W_B(U_{10})$ is the fractional coverage of Stage-B whitecaps. Monahan and O'Muircheartaigh (1980) gave

$$W_B(U_{10}) = 3.84 \times 10^{-6} U_{10}^{3.41}, \tag{19}$$

which gives the fraction of the sea surface covered by decaying whitecaps when U_{10} is in m s^{-1}.

Since we are interested in the evolution of spray droplets from the instant they form, a spray generation function that is in terms of r_{80} needs modification. Andreas (1989, 1992) showed that

$$\frac{\mathrm{d}F_W}{\mathrm{d}r_0} = \frac{\mathrm{d}r_{80}}{\mathrm{d}r_0}\frac{\mathrm{d}F_W}{\mathrm{d}r_{80}}, \tag{20}$$

where

$$r_{80} = 0.518 r_0^{0.976}, \tag{21}$$

derives from Fitzgerald's (1975) work and relates r_{80} and r_0. Thus,

$$\frac{\mathrm{d}r_{80}}{\mathrm{d}r_0} = 0.506 r_0^{-0.024}. \tag{22}$$

In Equation (20), $\mathrm{d}F_W/\mathrm{d}r_0$ is the spray droplet number flux per m^2 of sea surface per sec per μm increment in r_0, the droplet radius at formation. Equation (20) is valid for $0.5 \leq r_{80} \leq 12$ μm and for $1 \leq U_{10} \leq 20$ m/s.

Figure 3 shows examples of the spray generation function developed by Woolf *et al.* (1988) plotted as the volume flux $(4\pi/3)r_0^3(\mathrm{d}F_W/\mathrm{d}r_0)$, because this is the crucial term for spray heat transfer.

Blanchard (1963) was one of the first to estimate the spray generation function. Using the sea-salt distributions that Woodcock (1953) had measured at an altitude of 600 m in the marine boundary layer near Hawaii, Blanchard deduced the spray generation function for wind speeds between 5 and 15 m/s. Later, Gathman (1982) fitted Blanchard's curves with mathematical functions and programmed them into the Navy aerosol model.

Because Blanchard's (1963) and Gathman's (1982) way of expressing the spray generation function is not directly compatible with most of the other published functions, we present here a mathematically modified version of the

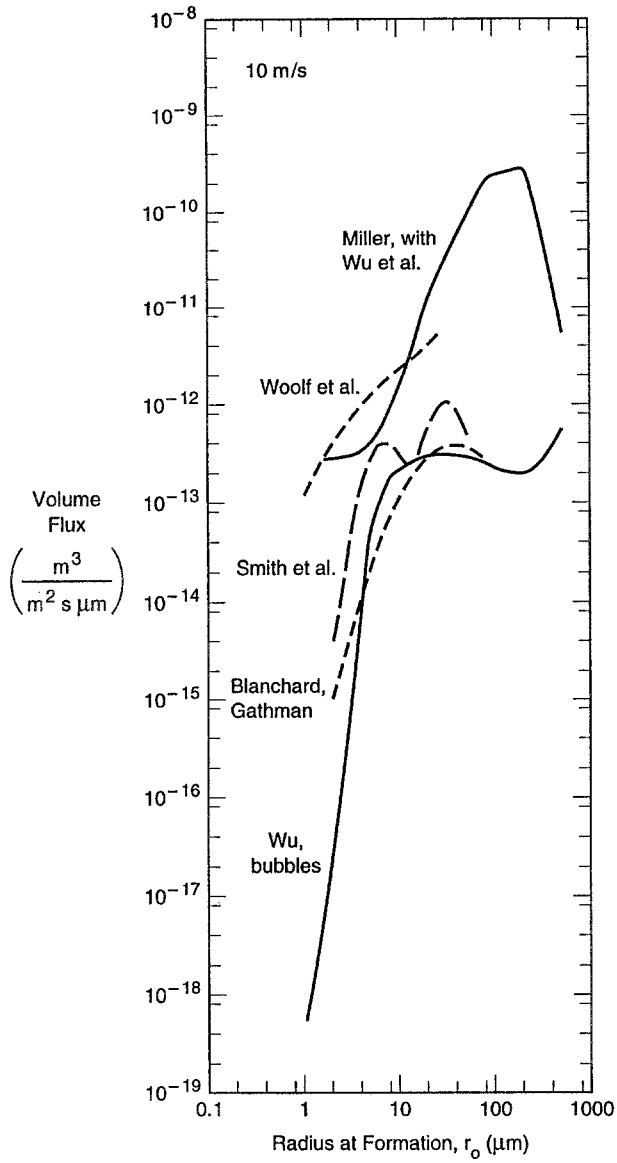

Fig. 3a.

Blanchard-Gathman function. Woodcock (1953) made his observations at a relative humidity of 91.4%; hence, in the Blanchard-Gathman model, all droplet radii are specified at this humidity. Our modified version of Gathman's prediction equation is

$$\frac{dF_{BG}}{dr_{91.4}} = \frac{2.152 \times 10^4 C_2}{r_{91.4}} \exp\left\{C_3\left[\ln\left(\frac{C_4}{r_{91.4}}\right)\right]^2\right\}. \tag{23}$$

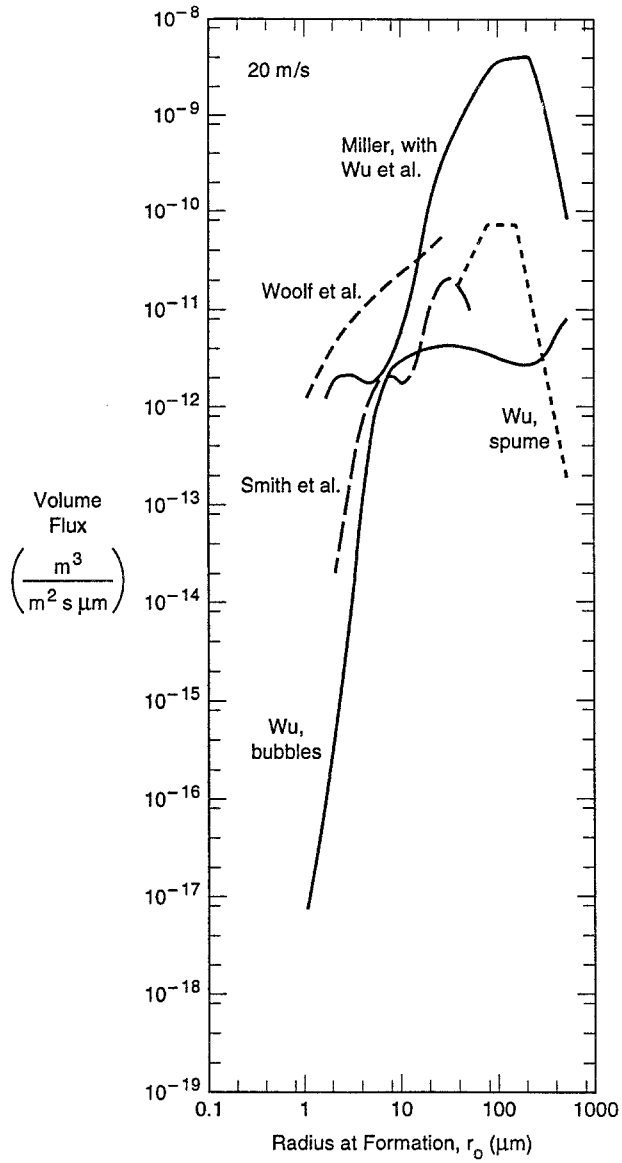

Fig. 3b

Fig. 3. Various models for the sea spray generation function at 10-m wind speeds of 10 ms (a) and 20 m/s (b). The models depicted are from Blanchard (1963), with Gathman's (1982) analytical fit; Woolf *et al.* (1988); Miller (1987), with the large-droplet extension based on Wu *et al.* (1984) (Andreas, 1992); Wu (1992, bubbles); Smith *et al.* (1993); and Wu (1993, spume).

This, as before, gives the number of spray droplets produced per m^2 of surface area per sec per μm increment in $r_{91.4}$, the droplet radius (in μm) of a spray droplet at a reference relative humidity of 91.4%. In Equation (23),

$$C_2 = 10^{-3}[-7.34 + 8.966(\ln U_{10})], \tag{24}$$

$$C_3 = -1.4301 + 0.07503U_{10}, \tag{25}$$

$$C_4 = 1.764 + 0.3713U_{10}, \tag{26}$$

where U_{10} is the 10-m wind speed in m s^{-1}.

As above, a spray generation function in terms of $r_{91.4}$ is not immediately useful. But we can convert $r_{91.4}$ to r_0 as we did before; that is,

$$\frac{dF_{BG}}{dr_0} = \frac{dr_{91.4}}{dr_0}\frac{dF_{BG}}{dr_{91.4}}, \tag{27}$$

where, for a salintiy of 34‰,

$$r_{91.4} = 0.627r_0^{1.002}, \tag{28}$$

and

$$\frac{dr_{91.4}}{dr_0} = 0.628r_0^{0.002}. \tag{29}$$

The Blanchard-Gathman spray generation function is valid for r_0 between 2 and 80 μm and for U_{10} between 5 and 15 m/s.

Because Blanchard (1963) based his spray generation function on Woodcock's (1953) observations at 600 m, it can account for few, if any, of the spume droplets that are important in the air-sea transfer of sensible and latent heat. Nevertheless, Figure 3 shows that, 30 years after Blanchard developed it, that function is still not too different from modern estimates.

Miller (1987; see also Miller and Fairall, 1988; Fairall *et al.*, 1990a) devised a spray generation function that is the consensus of four oceanic data sets. Although Miller's model covers only spray droplets for which $0.8 \leq r_{80} \leq 15$ μm, Andreas (1992, 1994b) speculated that, because it was derived from near-surface oceanic observations, spume droplets contributed to the counts at the largest radii (e.g., Monahan *et al.*, 1983b). He, thus, matched the large-droplet size distributions measured by Wu *et al.* (1984) to Miller's model at $r_{80} = 15$ μm to create a spray generation function that explicitly treats spume production. Katsaros and de Leeuw (1994) and Andreas (1994b) discussed this procedure. Andreas (1992) gave the mathematical formulation of the entire function derived from Miller and Wu *et al.* Figure 3 shows examples of this spray generation function.

Recently, Wu (1992) predicted the spray generation function by starting with the oceanic bubble spectrum, an approach that Fairall and Edson (1989) and de Leeuw (1990c) also described. His paper gives the necessary equations for computing the generation function, with one exception; his Equation (12) contains two errors. Wu used this equation to predict the terminal rise speed of dirty bubbles, w_d; with corrections, his Equation (12) can be written

$$\frac{3C_D w_d^2}{4D}\left(\frac{\rho_s}{\rho_s - \rho_a}\right) = g. \tag{30}$$

Here, ρ_s and ρ_a are the sea water and air densities, C_D is the drag coefficient of a dirty bubble with diameter D, and g is the acceleration of gravity.

Because in Wu's (1992) model the spray results from bursting bubbles only, his model does not treat spume production. Therefore, for winds of Beaufort Force 5 and higher, and for droplets with r_0 greater than 20 μm, Wu's model is not accurate. Figure 3 shows examples of Wu's spray generation function.

Smith *et al.* (1993) determined the spray generation function from aerosol concentration measurements on the island of South Uist in the Outer Hebrides. They made their measurements 14 m above mean sea level on a tower located near the top of a windward beach. Their paper contains all the equations for computing their model function, $\mathrm{d}F_S/\mathrm{d}r_{80}$, where, again, r_{80} is the droplet radius at a reference relative humidity of 80%. Using (20)–(22) to convert $\mathrm{d}F_S/\mathrm{d}r_{80}$ to $\mathrm{d}F_S/\mathrm{d}r_0$, we show in Figure 3 examples of the spray generation function developed by Smith *et al.*

The wind speed range that $\mathrm{d}F_S/\mathrm{d}r_0$ covers, 1–34 m/s, is the widest of any spray generation function that we have found. Thus, it surely must reflect some spume production. Smith *et al.* (1993), nevertheless, speculated that, because they collected their data some distance from where the droplets were produced, they may underestimate the large-droplet component. Thus, Smith *et al.* cautioned that their function represents a lower limit for the spray flux.

Following the lead of Monahan *et al.* (1986) and Andreas (1992) in assuming that the spray generation function has the same radius dependence as the near-surface droplet concentration spectrum, Wu (1993) used his laboratory measurements (Wu, 1973) and the oceanic observations of Wu *et al.* (1984) to develop a spray generation function for spume only. His paper contains all the equations for computing that function. Because his model is appropriate only for 10-m winds between 14 and 24 m/s, we show it in the right panel of Figure 3 but not in the left panel. Although Wu's prediction seems to be in fair agreement with other functions at 20 m/s, we believe it cannot be accurate throughout its specified wind speed range because it has an exponential dependence on u_* rather than the near-cubic dependence that we predicted earlier. In fact, for a wind speed of 15 m/s, Wu's spume function predicts a smaller volume flux of large spray droplets than his generation function based on the oceanic bubble spectrum (Wu, 1992), a result that seems inconsistent.

The several spray generation functions plotted in Figure 3 show regions of good agreement and regions of obvious differences. For r_0 between 5 and 20 μm – predominantly the jet droplet region – all the functions plotted in Figure 3 agree within 1–2 orders of magnitude. At smaller radii, Wu's (1992) model predicts much smaller fluxes than the others do.

Only the function that Andreas (1992) derived from the work of Miller (1987) and Wu *et al.* (1984) spans the range of relevant droplet sizes and has realistic levels for radii larger than 30 μm – that is, in the spume domain (also, see Andreas, 1994b). As we explained, the models by Woolf *et al.* (1988) and

Wu (1992) completely ignore spume production, and the Blanchard (1963) and Gathman (1982) function derived from data collected well above the region where spume would predominate. The model that Smith *et al.* (1993) developed undoubtedly reflects some spume production; in Figure 3, their function does begin rising in the spume region, mirroring Miller's model. But because Smith *et al.* collected their aerosol data away from the immediate area where spume is produced, they suggested that their model underestimates the spray generation function at the larger radii. In the spume domain, all the functions in Figure 3 hint at the existence of a peak in the volume flux. Wu's (1993) function, in fact, peaks essentially in the same place as the function that Andreas derived from Miller and Wu *et al.* But these two results are not really independent because Wu also based his generation function on the concentration spectra that Wu *et al.* measured. Hence, the models that we have surveyed lead to no consensus on either the amplitude or the location of the peak in the spray generation function. Thus, for now, Andreas's function seems most useful; but the rate of spume production is still known to no better than ±50%.

The six models for the spray generation function that we have focused on are not the only estimates of this function. Ling *et al.* (1978, 1980; also Ling, 1993), Cipriano and Blanchard (1981), Fairall (Fairall *et al.*, 1983; Fairall and Larsen, 1984), and Bortkovskii (1987) also attempted to quantify spray production. We have not discussed these models in detail.*

4. How Droplet Evaporation Modifies Low-Level Water Vapor and Temperature Profiles

4.1. Processes near the sea surface

The generation of whitecaps and the injection of sea spray into the atmosphere creates a transition zone between air and sea (Roll, 1965); the air-sea interface is no longer a simply connected surface. Initially, the spray droplets have the same properties as the ocean surface. Immediately after forming, however, they begin to adapt to conditions in the ambient air. Though many of the droplets quickly fall back into the sea, a substantial proportion of the smaller ones evaporate entirely, leaving only dry salt particles. Turbulence can carry these up to cloud heights, where they are an important source of cloud condensation nuclei and, in fact, lead to a salt inversion just below cloud base (Blanchard and Woodcock, 1980). The resulting vertical distribution of droplets and sea salt also plays an

* The model by Ling et al. is somewhat unphysical and also yields production rates that seem to be several orders of magnitude too large (Fairall and Edson, 1989; Andreas, 1994b). Cipriano and Blanchard presented their results only graphically and incorporated no wind speed dependence; they are, thus, not comparable with the other models that we have discussed. The generation functions that Fairall et al. and Fairall and Larsen reported were forerunners of Miller's (1987) model. Bortkovskii's model also predicts too many droplets (Andreas, 1994b) and contains an adjustable parameter, the mode droplet radius, for which we do not have a good, independent prediction when spume becomes important.

important role in determining the optical properties of the marine atmosphere (Davidson and Fairall, 1986).

It has long been postulated that evaporating spray droplets influence the surface energy budget of the ocean (Montgomery, 1940). During their transport through the atmosphere, the droplets are sources or sinks of sensible heat, moisture, and latent heat. However, the nature of the numerous interactions between the droplets and the air-sea system is complex and poorly understood. To better understand the influence of sea spray on the near-surface energy budget, several recent research programs have studied these interactions. One of these, the HEXOS program (Humidity Exchange Over the Sea), set out specifically to investigate the effects of evaporating spray on the near-surface energy budget through a combination of numerical modelling, laboratory simulations, and open-ocean measurements (Katsaros *et al.*, 1987; Smith *et al.*, 1990). These measurements have validated parameterizations used in several recently developed numerical models of spray diffusion.

4.2. Impact of droplet evaporation on heat and moisture transfer

In the absence of rain, snow, fog, or sea spray, all of the air-sea fluxes of moisture and latent heat originate with surface evaporation and result in a loss of heat from the ocean. Under these same conditions, when the air is cooler than the sea, an upward sensible heat flux originating at the sea surface also cools the ocean (Fairall and Edson, 1989). These surface heat fluxes and the momentum flux, or surface stress, τ, are constants within an atmospheric surface layer that extends up to about one-tenth the height of the marine boundary layer.

When spray droplets are present, however, their evaporation and cooling cause the heat fluxes to vary with height near the sea surface. Within a 'droplet evaporation layer' (DEL; Smith, 1989, 1990), droplets cool by two processes. First, since they start at the temperature of the sea surface, if the sea is warmer than the air, they cool by losing sensible heat to the air. Second, they cool by evaporation. Because the thermal equilibrium time of droplets, τ_T, is much shorter than their evaporative equilibrium time, τ_r (Figure 2), the latent heat they consume in evaporating is accompanied by a nearly equal sink of sensible heat. Clearly, since spray droplets are elevated sinks and sources for heat and moisture, the scalar fluxes can no longer be constant with height in the DEL (e.g., Ling and Kao, 1976; de Leeuw, 1990b).

With spray droplets acting as elevated sources of moisture and sinks for heat, the near-surface air is cooler and moister than it would be in the absence of droplets (Mestayer and Lefauconnier, 1988). Consequently, there should be reduced latent heat loss at the air-sea interface and an enhanced upward flux of sensible heat at the interface.

Assuming neutral stratification, we can describe the influence of evaporating droplets on the scalar fluxes and on the profiles of potential temperature (θ) and

specific humidity (q) near the sea surface by the classical flux-gradient formulas (e.g., Donelan, 1990),

$$\frac{\mathrm{d}q}{\mathrm{d}z} = \frac{q_*(z)}{\kappa z}, \tag{31}$$

$$\frac{\mathrm{d}\theta}{\mathrm{d}z} = \frac{t_*(z)}{\kappa z}, \tag{32}$$

where κ is again von Kármán's constant. Here, however, the scaling parameters for humidity and temperature flux, $q_*(z)$ and $t_*(z)$, must vary with height, since the heat fluxes do. Nevertheless, we still relate these parameters to the sensible (H_s) and latent (H_L) heat fluxes, as usual;

$$H_s(z) = -\rho_a c_p u_* t_*(z), \tag{33}$$

$$H_L(z) = -\rho_a L_v u_* q_*(z), \tag{34}$$

where c_p is the specific heat of air at constant pressure, and L_v is the latent heat of vaporization of water. In the absence of spray, or outside the DEL, H_s, H_L, t_*, and q_* would be constants with height, and Monin–Obukhov similarity obtains.

Smith (1990) proposed, for purposes of illustration, a DEL between heights $Z1$ and $Z2$ in which droplet evaporation S_q is uniform, $S_q(z) \simeq S_q$ (in g water vapor per m^3 per sec). As a result, the latent and sensible heat fluxes vary linearly with height here (Figures 4 and 5), while below $Z1$ and above $Z2$, the fluxes are constants with height. The lower constant-flux layer, between the surface and $Z1$, is so thin that droplet evaporation here has negligible influence, even though this layer may span several decades on a logarithmic scale. The height $Z1$ may correspond to the spray droplet ejection height – roughly 10–20 cm. The upper height $Z2$ is a level above which there is no significant evaporation. We suggest later that $Z2$ scales with $A_{1/3}$. This distinct layering is, of course, a simplification; in reality, the layers would have fuzzy edges.

Smith (1990) hypothesized that, at any level, the turbulent moisture and sensible heat fluxes, regardless of their sources, determine the vertical gradients of humidity and temperature at that level. That is, the fluxes and gradients are 'locally ignorant' of the sources and sinks of heat and moisture in overlying and underlying layers; then Equations (31) and (32) are valid locally, even at heights within the layer where evaporating droplets are sources and sinks of latent and sensible heat. Figures 6 and 7 are humidity and temperature profiles that would, thus, be associated with the respective flux profiles in Figures 4 and 5.

This local ignorance hypothesis is mathematically analogous to the local similarity hypothesis (Nieuwstadt, 1984; Sorbjan, 1986) that has been used successfully to treat stable boundary layers. In a stable boundary layer, vertical exchange is restricted; as a consequence, elevated layers may have no direct communication

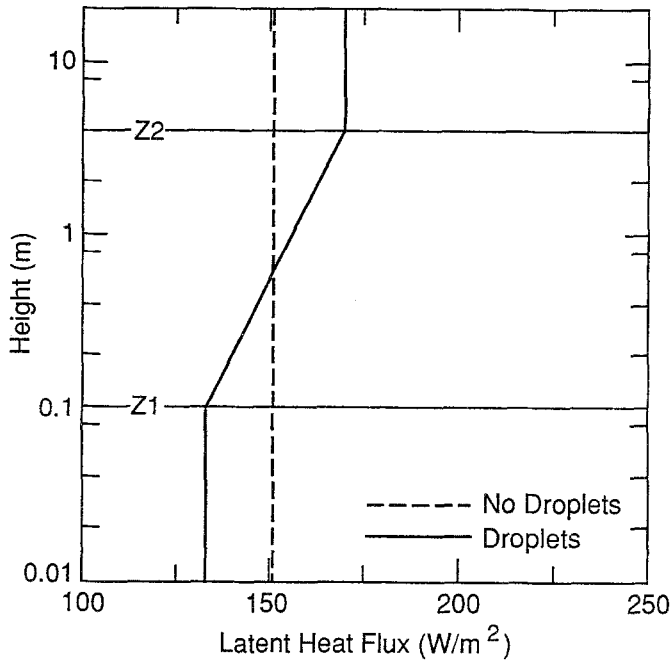

Fig. 4. Hypothetical turbulent latent heat flux profile assuming uniform evaporation between levels $Z1$ and $Z2$ (solid line). Here, $u_* = 0.35$ m/s, and $Z1$ and $Z2$ were chosen arbitrarily to delimit a typical droplet evaporation layer. The dashed line shows the latent heat flux profile in the absence of droplets.

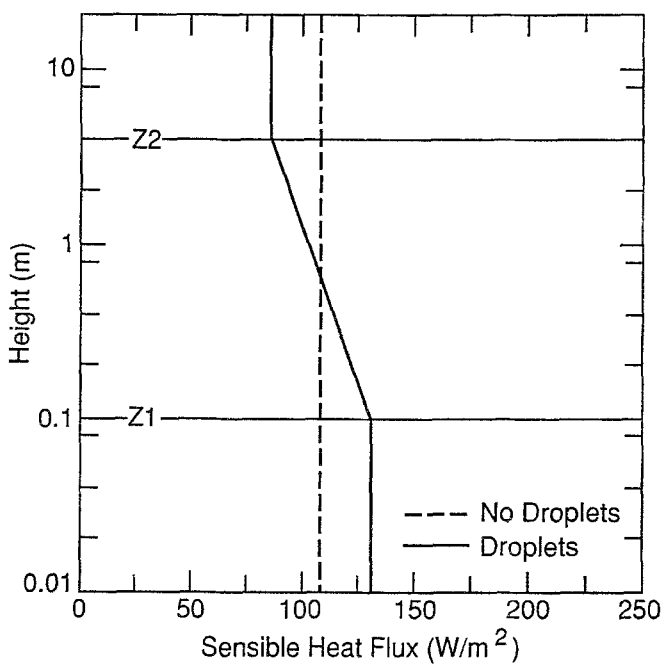

Fig. 5. Same as Figure 4, except these are turbulent sensible heat flux profiles.

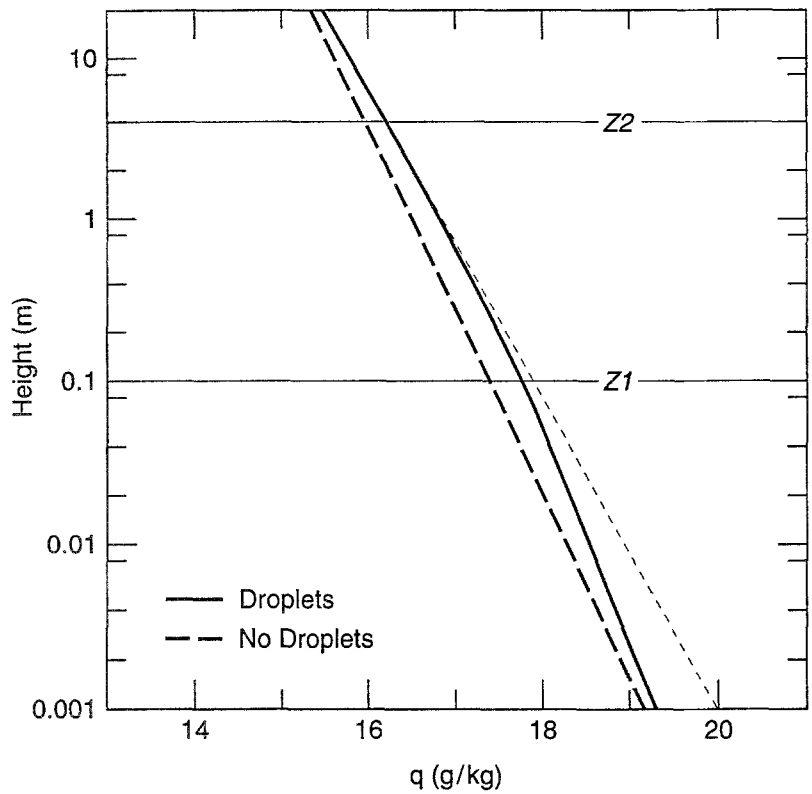

Fig. 6. Hypothetical vertical specific humidity profiles associated with the flux profiles in Figure 4. The dotted line shows how the constant-flux profile above $Z2$ would be extrapolated to the surface.

with the surface. Thus, their properties cannot scale with the surface values of the momentum and heat fluxes, the traditional scales of Monin–Obukhov similarity. Rather, the local values at height z are more meaningful scales. Similarly, in the DEL, the elevated sources and sinks of heat and moisture obscure information about the surface fluxes. Again, the local fluxes at height z provide better flux scales than quantities derived from the surface fluxes. Our one difference with local similarity is that we need not assume that u_* changes with height; spray concentrations are so low that the spray seems to have no effect on the dynamics of the flow (Wu, 1979b).

At any level z, the turbulent vapor flux is the rate of evaporation at the surface plus the integral of droplet evaporation at levels below z. Below $Z2$, there is also a net upward transport of liquid water in droplets. Because u_* is constant with height, the variation of vapor flux is accompanied by a proportional variation in

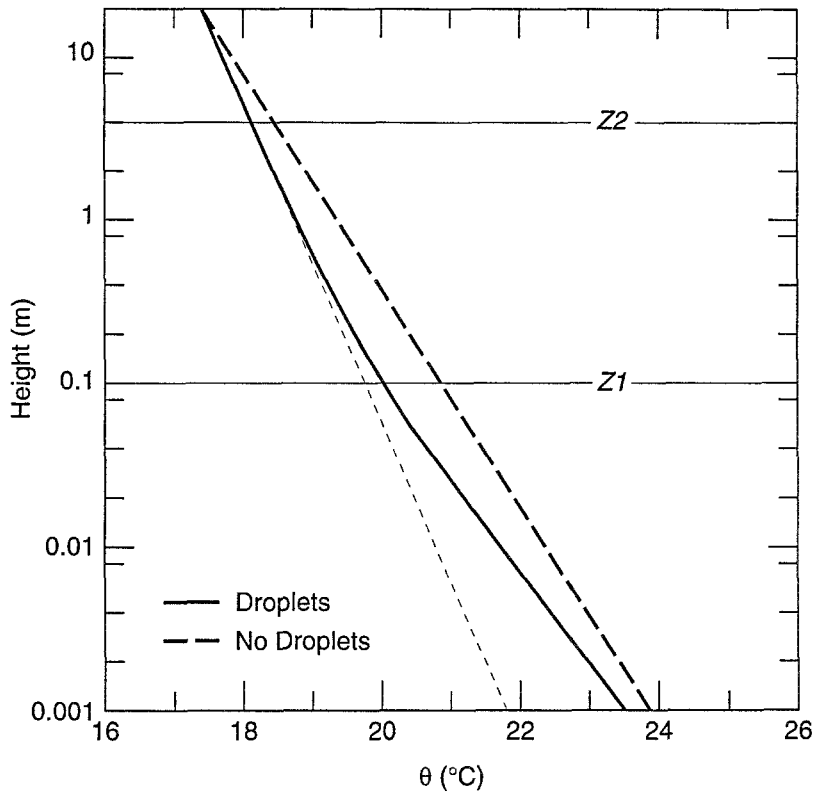

Fig. 7. Hypothetical vertical potential temperature profiles associated with the flux profiles in Figure 5. The dotted line shows how the constant-flux profile above $Z2$ would be extrapolated to the surface.

q_*. For $Z1 \leq z \leq Z2$, $q_*(z)$ is simply (noting that q_* is negative for an upward vapor flux)

$$q_*(z) = q_{*s} - \frac{1}{\rho_a u_*} \int_{Z1}^{z} S_q(z)\, \mathrm{d}z \simeq q_{*s} - \frac{(z - Z1) S_q}{\rho_a u_*}, \tag{35}$$

where q_{*s} is the value of the flux scale at the surface (same value as at $Z1$). Remember, $q_*(z)$ dictates the slope of the humidity profile within the DEL (see Equation (31) and Figure 6). Dashed lines in Figures 4 and 6 indicate the constant latent heat flux and the associated logarithmic humidity profile in the absence of droplet evaporation. But when spray is present, the turbulent vapor flux is reduced in the near-surface layer, $z \leq Z1$, and increased in the layer above $Z2$ (Figure 4). The latter increase is the net influence of droplet evaporation on the atmosphere.

By the local ignorance hypothesis, the structure of the boundary layer for $z > Z2$ is unaffected by – is ignorant of – the distribution of vapor sources in lower layers. The structure of the constant-flux layer above $Z2$ is, therefore, identical

to the structure of a classical constant-flux surface layer without evaporating droplets but with a modified humidity roughness length z_q (see the dotted line in Figure 6).

Evaporation cools the droplets and the air in the DEL. Droplet effects on the sensible heat flux within the DEL are not as easy to understand because these droplets also influence the temperature profile through the sensible heat they carry. In a subsequent section, we estimate, however, that the latent heat flux associated with evaporating droplets is often an order of magnitude larger than the sensible heat they exchange. Thus, ignoring this sensible heat exchange, we can approximate the influence on the temperature profile of the latent heat that droplets consume by using an argument similar to that above (compare Figures 4 and 5).

The sensible heat flux at level z is the surface flux plus the integral of the sink from evaporating droplets between $Z1$ and z. That is, for $Z1 \leq z \leq Z2$ (noting that t_* is negative for an upward sensible heat flux),

$$t_*(z) = t_{*s} + \frac{L_v}{\rho_a c_p u_*} \int_{Z1}^{z} S_q(z)\, \mathrm{d}z \simeq t_{*s} + \frac{L_v(z - Z1)S_q}{\rho_a c_p u_*}. \tag{36}$$

$t_*(z)$ also gives the slope of the temperature profile (see Equation (32) and Figure 7). The heat sink in the DEL, in effect, reduces the net sensible heat flux above height $Z2$. By the local ignorance principle, the distribution of sources and sinks of sensible heat in underlying layers does not influence the structure of the constant-flux layer above height $Z2$; it is, thus, identical to a classical boundary layer with a modified temperature roughness length z_t (see the dotted line in Figure 7).

One way of viewing the water vapor derived from droplets is to somehow tag it separately from the vapor coming from the surface and to consider it as a perturbation on the existing structure. (This viewpoint is less valid for large perturbations that affect the stratification.) To maintain a steady state, the tagged vapor must escape from the DEL, traveling up or down by eddy diffusion away from the maximum of tagged humidity. If, for example, the eddy diffusivity for the flux of tagged vapor away from the DEL were the same in the upward and downward directions, half of the water evaporated from droplets would travel upward and the other half would travel downward. The tagged vapor that travels down causes a negative feedback by reducing the vapor flux in the layer between the surface and $Z1$; the vapor that travels up enhances the net flux above $Z2$.

The dashed line in Figure 5 represents the sensible heat flux in the absence of droplets. If the eddy diffusivities above and below the DEL are the same for sensible heat and water vapor (or even in the same ratio), the reduction in sensible heat flux above height $Z2$ is the same as the enhancement of latent heat flux there. Consequently, droplet evaporation would not alter the total turbulent (sensible plus latent) heat transferred to the atmosphere above $Z2$. Likewise, the

total turbulent heat transport between $Z1$ and the surface is unaltered, as is the heat taken from the upper ocean.

This partitioning between turbulent and spray fluxes can also be determined experimentally. In HEXMAX (the HEXOS Main Experiment), Katsaros and DeCosmo (1993) and DeCosmo *et al.* (1994) found, from eddy fluxes measured at a height of about 7 m, that C_E, the bulk transfer coefficient for water vapor, did not increase significantly with wind speed for speeds up to 18 m/s. In other words, for these wind speeds, the evaporation from droplets did not seem to enhance the measured net flux at this level by more than about 15%, the uncertainty in the measurements. Three conclusions are possible. First, the evaporation from droplets is not significant for wind speeds up to 18 m/s. Second, most of the vapor from evaporating droplets is transported back down to the surface. Third, at the higher wind speeds, the instruments were within the DEL (i.e., $Z2 > 7$ m); thus, the measured vapor flux was less than the net flux above $Z2$. We shall show in a later section that this third alternative is likely for winds above 15 m/s.

We could also extend the above approach to include the sensible heat exchanged by droplets by postulating a sensible heat transfer layer (SHL), where the droplets exchange their sensible heat with the air. But because the heat consumed by evaporating droplets will likely exceed this sensible heat, we do not have as good a conceptual picture for the disposition of sensible heat as we do for the tagged water vapor. Because the thermal equilibrium time scale, τ_T, is much shorter than the moisture equilibrium time scale, τ_r (Figure 2), the SHL may also not have the same height limits as the DEL.

4.3. Numerical modelling

The turbulent transport of heavy particles in the atmospheric boundary layer is an interesting and a difficult field of study. Trying to properly model the turbulent field responsible for transporting these particles and their resulting response in it is one of the problems that has interested us. The response of heavy particles is governed by their inertia and their gravitational settling, both of which depend on their size, shape, and density. These processes are, of course, interrelated, which complicates their parameterization.

Attempts to model the vertical distribution of sea-salt aerosols began shortly after Woodcock's (1953) study provided data on their vertical distribution as a function of wind speed. These models include the pioneering works of Junge (1957), Eriksson (1959, 1960), and Toba (1965a, 1965b, 1966). Recently, several Eulerian models have successfully treated the turbulent diffusion of discrete particles in boundary-layer flows. These include the studies of Ling and Kao (1976), Ling *et al.* (1978, 1980), Ling (1993), Burk (1984), Mostafa and Mongia (1987), Stramska (1987), and Rouault *et al.* (1991).

4.3.1. Eulerian Models

Stramska (1987) developed a dispersion model using K theory to close the following set of equations:

$$\frac{\partial N}{\partial t} = \frac{\partial}{\partial z}\left(K\frac{\partial N}{\partial z}\right) + \frac{\partial (w_s N)}{\partial z}, \tag{37}$$

$$\frac{\partial q}{\partial t} = \frac{\partial}{\partial z}\left(K\frac{\partial q}{\partial z}\right) + S_q, \tag{38}$$

$$\frac{\partial T}{\partial t} = \frac{\partial}{\partial z}\left(K\frac{\partial T}{\partial z}\right) - S_T. \tag{39}$$

Here, N is the number concentration of droplets with dry radius $1 \leq r_d < 15$ μm, q is the specific humidity, T is the air temperature, K is the turbulent diffusivity, and w_s is the Stokes fall speed. (Note, $2r_d \simeq r_{80}$; $2r_{80} \simeq r_0$.) S_q and $S_T = L_v S_q / c_p$ represent sources of water vapor and sensible heat, respectively.

The model does not attempt to simulate the actual ejection of the droplets; its main focus is on examining the influence of evaporating droplets in the atmospheric surface layer rather than their near-surface structure. The model assumes that the droplets instantaneously reach their equilibrium size for the given ambient humidity. The moisture given up as a result of this process is modelled using

$$S_q = \sum_{r_d} \frac{1}{\rho_a}\frac{\partial m_d}{\partial z}\left(K\frac{\partial q}{\partial z} + w_s q\right), \tag{40}$$

which describes the competing processes of turbulent diffusion and gravitational fallout in extracting water vapor from evaporating droplets. Here, m_d is the mass concentration of spray droplets of radius r_d. The ejection of droplets into the model domain is determined by the flux of droplets at the surface using the spray generation function developed by Monahan *et al.* (1983a). Stramska (1987) modelled the additional source of moisture from the evaporation of larger droplets using an *ad hoc* droplet profile based on Preobrazhenskii's (1973) droplet size distributions and a logarithmic decrease in the vertical.

The programs HEXIST (HEXOS EXperiment In the Simulation Tunnel) and CLUSE (Couche Limite Unidimensionnelle Stationaire d'Embruns) were designed to investigate the generation, turbulent transport, and evaporation of droplets ejected by bursting bubbles within the air-sea simulation tunnel at the Institut de Mécanique Statistique de la Turbulence (IMST), Luminy, France. The setup used during CLUSE approximated the desired one-dimensional, stationary droplet boundary layer (S. D. Smith *et al.*, 1990; Rouault *et al.*, 1991). The measurements conducted during these experiments were used to develop two numerical models of droplet diffusion.

The first of these is the model that Rouault *et al.* (1991) developed, which looked at the behavior of droplets close to the surface. In their model, the fluid

is considered a multiphase mixture of dry air, water vapor, and I-categories of liquid droplets such that the mixture concentration is given by

$$\rho = \rho_a + \rho_v + \sum_{n=1}^{I} \rho_n, \tag{41}$$

where ρ is the mass concentration per unit volume, and the subscripts a, v, and n refer to air, water vapor, and the droplet concentrations, respectively. The variable describing the droplet concentration in their model is related to Stramska's (1987) by $\rho_n = (4\pi\rho_w r_n^3/3)N$, where ρ_w is water density. Also, $\rho_v = \rho_a q$. Droplet category n is defined by $r_n - 0.5\ \mathrm{d}r_n < r \leq r_n + 0.5\ \mathrm{d}r_n$, where the radius increment $\mathrm{d}r_n$ is 5 μm, and the droplet radii range from 10 to 100 μm (i.e., $I = 20$) in the latest version.

Although their budget equations were similar to Stramska's (1987), they modified them to allow for a discrete size distribution of jet droplets; that is,

$$\frac{\partial\langle\rho_a\rangle}{\partial t} = 0, \tag{42}$$

$$\frac{\partial\langle\rho_n\rangle}{\partial t} = \frac{-\partial\langle w_n'\rho_n'\rangle}{\partial z} - \frac{\partial\langle W_n\rangle\langle\rho_n\rangle}{\partial z} + S_n, \tag{43}$$

$$\frac{\partial\langle\rho_v\rangle}{\partial t} = \frac{-\partial\langle w'\rho_v'\rangle}{\partial z} + S_v. \tag{44}$$

In these, angle brackets indicate averaging, horizontal homogeneity is assumed, primes denote deviations from the means, and the source of water vapor (S_v) is solely from evaporating droplets such that

$$S_v = -\sum_{n=1}^{I} S_n. \tag{45}$$

The net source term for droplet concentration (S_n) models the effect of evaporation. It also provides the means by which the droplets move from one category to the next as they evaporate. An equivalent term in Stramska's model is not necessary because it explicitly treats only one category (i.e., $I = 1$, $\mathrm{d}r_n = 14$ μm, and $r_n = 8$ μm). Lastly, to determine how evaporating droplets influence the temperature field, the sensible heat budget equation,

$$\frac{\partial\langle T\rangle}{\partial t} = \frac{-\partial\langle w'T'\rangle}{\partial z} + \frac{L_v}{\rho_a c_p}\sum_{n=1}^{I} S_n, \tag{46}$$

is also allowed to converge simultaneously with the above expressions. A shortcoming of both models is that they do not include the source (sink) term Q_S

resulting from sensible heat release (consumption) by the spray droplets, which we describe in Section 5.

The mean droplet velocity $\langle W_n \rangle$ can be approximated by the mean fall speed. However, since one of the objectives of their model was to describe the behavior of jet droplets close to the surface, Rouault *et al.* (1991) chose to break up the fall speed into components that describe both the droplet's ejection from the surface and its tendency to fall back to the surface because of gravity. Similarly, the droplet flux at the surface is the sum of the ejected flux (i.e., the source function multiplied by the ejection velocity) and the deposition flux.

The turbulent fluxes of water vapor and droplets are also modelled using K-theory. The key difference between the two models is in their parameterization of droplet diffusion. Rouault *et al.* (1991) included a parameterization for the 'counter-diffusivity' resulting because a droplet's inertia prevents it from following the turbulent motions exactly. Therefore, the velocity fluctuation in (43) comprises the fluid velocity fluctuation plus a slip velocity, i.e., $w'_n = w' + \delta w'_n$. The droplet diffusion term is then defined by deriving an additional diffusivity to model this additional flux such that

$$\langle \rho'_n w'_n \rangle = -(K_n + K'_n) \frac{\partial \langle \rho_n \rangle}{\partial z}, \tag{47}$$

where K'_n comes from the work of Meek and Jones (1973). Including this term becomes increasingly important for a realistic description of droplet dispersion as droplet size increases.

4.3.2. Eulerian Model Results

Stramska's (1987) model is best suited for small droplets above the ejection layer, where the competing processes of turbulent diffusion and gravitational settling are responsible for droplet transport. The droplets must be small because the model does not take into account their inertial response. The largest dry radius used in the model, 15 μm, is a reasonable upper limit, based on Edson's (1989) numerical studies. Stramska's results indicate that the evaporation of sea spray droplets having dry radii less than 15 μm ($r_0 < 60$ μm) has little effect on the profiles of temperature and humidity. However, the model calculations for larger droplets, using the parameterization based on Preobrazhenskii's (1973) measured size distributions, show substantial modification to the scalar profiles for a wind speed of 20 m/s.

The results from the second model (Rouault *et al.*, 1991; Rouault and Larsen, 1990) show that within the DEL, droplets with radii of 15 to 40 μm contribute most to the water vapor produced by evaporating droplets (Figure 8). We obtain a similar result in Section 5 with an analytical model. Larger droplets have a higher fall speed (i.e., short τ_f) and disappear rapidly. Moreover, they are less likely to be transported by the turbulence to a more evaporative location. Since

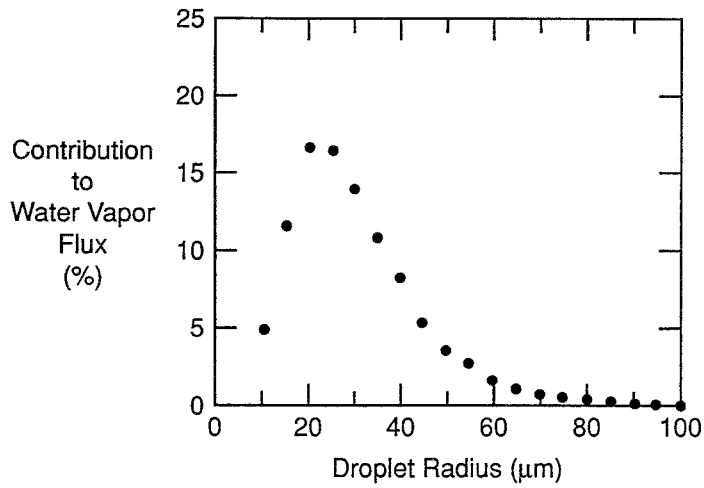

Fig. 8. Relative contribution of each S_n term to the increase in water vapor flux caused by spray evaporation, according to Rouault and Larsen's (1990) model. The simulated conditions correspond to those encountered during CLUSE: $u_* = 0.38$ m/s, $T_w = 20°C$, $T_a(z = 2\text{ m}) = 26°C$, $q(z = 0) = 12.6$ g/kg, and $q(z = 2\text{ m}) = 14.5$ g/kg (relative humidity of 69%). Each data mark is centered in a radius bin 5 μm wide.

a droplet's mass is proportional to r^3, the role of smaller droplets in evaporation from the sea is insignificant, as Stramska (1987) also concluded.

The area of maximum water vapor production and evaporative cooling is the ejection zone for jet droplets (between 1 and 15 cm). (The model does not specifically treat spume droplets.) Figures 9 and 10 show that the difference between the water vapor flux in the presence and absence of droplets has opposite signs above and below this zone. This result agrees with the proposed adjustments to the flux profiles that we described earlier; the principal difference is the height of the crossover point in the flux comparisons. The heights in Figures 4 through 7 were chosen arbitrarily only for demonstration purposes; over the ocean, the flux-crossover point in Figure 10 will be significantly higher because of waves and the generation of spume droplets.

The most important result here is that the influence of spray droplets is small at wind speeds less than 10 m/s, where the modification of the evaporative fluxes is at most 15% in a very evaporative case. However, using Bortkovskii's (1987) spray generation function resulted in a modification to the fluxes of as much as 100% for wind speeds greater than 15 m/s (Figures 9 and 10). Though we now believe that the Bortkovskii generation function overestimates the droplet production (Andreas, 1994b), when Rouault and Larsen (1990) developed their model, Bortkovskii's was the only reasonable spray generation function available with which they could study processes over the open ocean. Since Bortkovskii's function predicts roughly 100 times more spray production at its peak than the function that Andreas (1992) developed, we infer from Figure 10 that, with

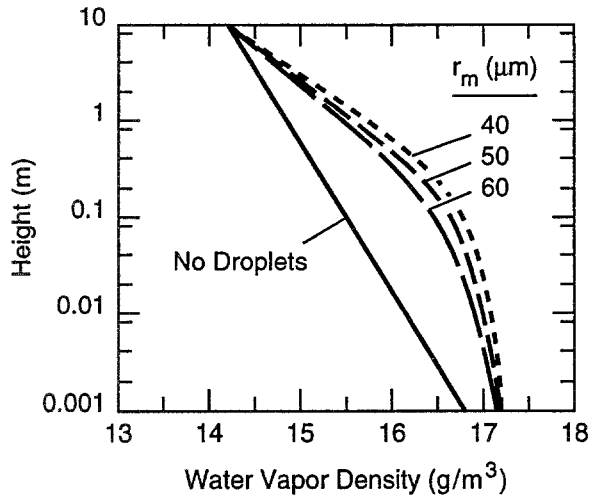

Fig. 9. Rouault and Larsen's (1990) model calculations of the vertical profile of the absolute humidity, ρ_v, using Bortkovskii's (1987) source function. The simulated conditions are for a 15-m/s wind speed (which corresponds to $u_* = 0.54$ m/s), $T_w = 20°C$, $T_a(z = 10 \text{ m}) = 25°C$, $q(z = 0) = 12.6$ g/kg, and $q(z = 10 \text{ m}) = 14.5$ g/kg (relative humidity of 73%). The solid line is the result for no droplets. The broken lines correspond to values of the mode radius (r_m) of 40, 50, and 60 μm. The mode radius is necessary in the Bortkovskii source function and corresponds to the radius where the maximum in the droplet volume spectrum occurs.

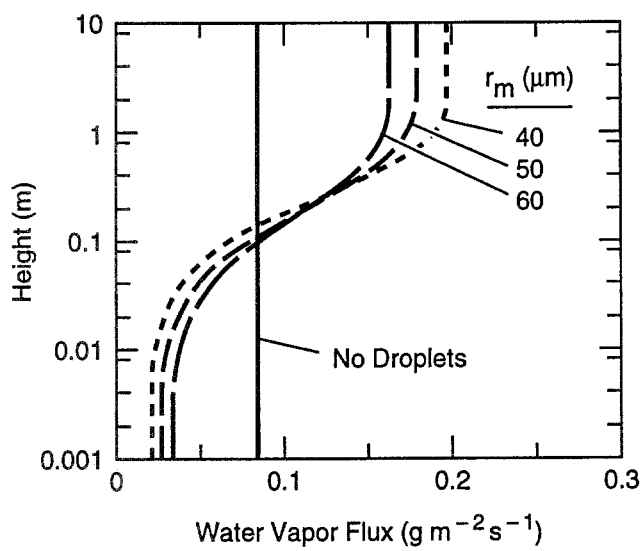

Fig. 10. As in Figure 9, except these are vertical profiles of the water vapor flux.

more realistic spray production, Rouault and Larsen's model would predict an enhancement in the water vapor flux of a few percent in a 15-m/s wind. We

therefore conclude that, for winds higher than 15 m/s, sea spray begins to have a measurable effect on the air-sea fluxes.

4.3.3. Lagrangian Models

Because it permits more flexibility in specifying boundary conditions, Lagrangian modelling has advantages over Eulerian modelling for studying heavy particles with low concentration, dispersing from a discrete source or in fluid flows with complicated geometries (e.g., near a wavy surface). For example, a Lagrangian scheme could simulate both jet and spume droplets; the spray generation function could be broken into the individual jet and spume components, with the jet droplets ejected more or less uniformly over the surface and the spume droplets ejected only at the wave crests.

Edson and Fairall (1994) described a Lagrangian model based on a Langevin equation modified to account for gravitational and inertial effects. The model, a Lagrangian simulation of turbulently transported jet droplets ejected by bubbles bursting at the surface, was tested using measurements made during the HEXIST and CLUSE experiments. Briefly, the model assumes that the motion of the droplet is steady-state so that its velocity consists of a mean plus a fluctuating component that is modeled with a Langevin equation. The finite difference form of the Langevin equation for a droplet's vertical velocity is then

$$W^d(t+\Delta t) = \left(1 - \frac{\Delta t}{\tau_w^d}\right) W^d(t) + \sigma_w^d \left(\frac{2}{\tau_w^d}\right)^{1/2} \xi(t) + \frac{\Delta t}{\tau_w^d} \overline{W^d}. \tag{48}$$

Here, τ_w^d is the droplet integral time scale, σ_w^d is the standard deviation of the droplet's vertical velocity, $\overline{W^d}$ is the droplet's average vertical velocity, and $\xi(t)$ is a random number drawn from a Gaussian distribution with zero mean and variance Δt using a technique based on the Central Limit Theorem.

Edson and Fairall (1994) used the following expression for the droplet's vertical velocity variance:

$$(\sigma_w^d)^2 = \frac{\sigma_w^2}{(1+\chi)}, \tag{49}$$

where σ_w^2 is the vertical velocity variance of the turbulent fluid. Here, also, χ is the ratio of the droplet response time to the Lagrangian integral time scale, τ_L. This parameter determines how the droplet reacts to the turbulent motion of the surrounding fluid. For example, when the droplet encounters smaller eddies as it nears the surface, the influence of the turbulence on the droplet motion diminishes because the droplet can no longer react to these smaller eddies. The droplet's size determines the height at which this begins to occur.

Figure 11 shows sample calculations of σ_w^d for droplets ranging in radius from 10 to 130 μm. As we explained above, σ_w^d must be a function of height.

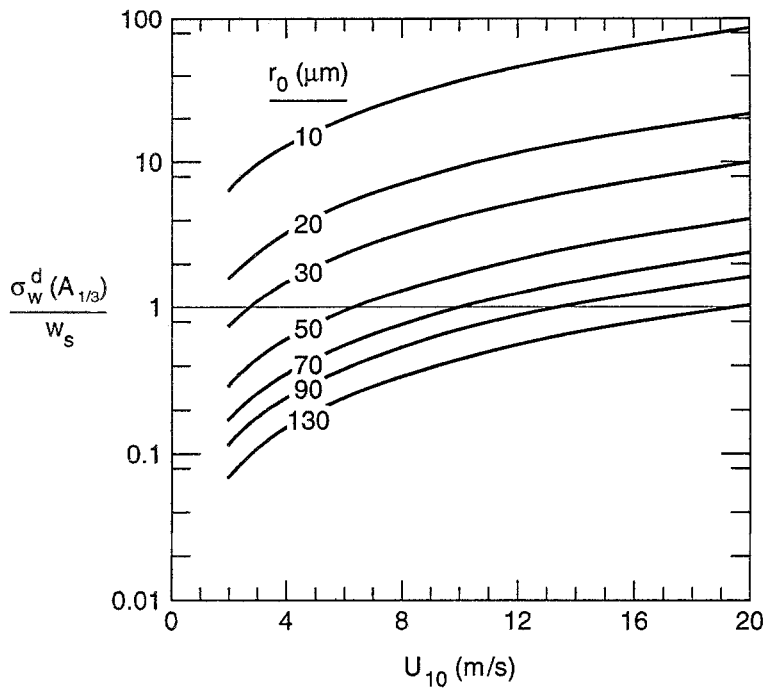

Fig. 11. Calculations of the standard deviation in vertical velocity, σ_w^d, for spray droplets of radius r_0, based on Edson and Fairall's (1994) Lagrangian model. σ_w^d is nondimensionalized by the droplet's terminal fall speed w_s and is evaluated at a height of $A_{1/3}$, where $A_{1/3}$ comes from Equation (11). U_{10} is the 10-m wind speed, and the calculations are for nonevaporating conditions.

Therefore, in the figure, σ_w^d is evaluated at one significant-wave amplitude above the surface and is made nondimensional with the terminal fall speed of the droplet, w_s. Our modelling has shown that turbulence cannot advect droplets away from the surface unless $\sigma_w^d/w_s > 1$. Figure 11, thus, corroborates our use of the droplet time scales discussed in Section 3.1 and depicted in Figure 2. Film droplets and most jet droplets require only a modest wind to be advected upward and thereby given enough time to exchange all of their moisture. In a 5-m/s wind, however, turbulence can advect only droplets at the small end of the spume domain. But as the 10-m wind increases, turbulence can carry larger and larger spume droplets away from the surface, giving them the chance to exchange their moisture.

The figure also agrees with our earlier statement that the threshold wind speed for spume production is in the 7–11 m/s range. Though the wind may be strong enough to rip a parcel of water from a wave crest, we would not say that spume was forming unless the turbulence intensity at the wave crests was also high enough to suspend the droplets formed. Without this turbulent suspension, they would fall right back into the sea. Figure 11 shows that, for winds of 7–11 m/s, the turbulence becomes intense enough to suspend droplets with radii of 50–80

μm. These are spume droplets in the size range just to the left of the peak in the spray generation function based on Miller (1987) and Wu *et al.* (1984) (see Figure 3).

The droplet integral time scale τ_w^d, a measure of persistence in the droplet's velocity as it moves through the fluid, is derived by determining the droplet's autocorrelation function in an approach similar to that used by Meek and Jones (1973). Integrating this autocorrelation function yields

$$\tau_w^d = \frac{\tau_L}{\Lambda}(1 + \chi), \tag{50}$$

where Λ accounts for the reduction in the correlation of the droplet's velocity between successive time steps because of gravitational fallout. In other words, this decrease in correlation results because the droplet 'falls out' of a fluid eddy whose motion is highly correlated.

To illustrate one use of such a model, we turn to a study reported by Edson (1990) that de Leeuw's (1986a, 1986b) measurements prompted. De Leeuw found a minimum in his droplet concentration profiles between 0.2 and 0.5 m and a maximum at 1–2 m for wind speeds greater than 7 m/s. Naturally, there is some debate as to what causes these extrema in the droplet concentrations (e.g., Wu, 1990d; de Leeuw, 1990a). Attempts have been made to explain these peculiarities through mechanisms such as jet droplet ejection, spume droplet production, and rotor-like features in the flow field that trap droplets (de Leeuw, 1986b, 1987, 1990b; Wu, 1990d). Edson investigated a few of these mechanisms with the above Lagrangian model.

Clearly, once the droplets are airborne, waves – through their influence on the velocity field (at least near the surface) – must affect droplet motion. Therefore, the model must somehow include wave effects if we wish to understand droplet concentration profiles over realistic seas. The resulting droplet profiles may also show how the droplets contribute to the sensible and latent heat fluxes (Fairall and Edson, 1989).

Including these effects in any model is extremely difficult because an accurate description of the velocity field over ocean waves depends on many factors that interact nonlinearly. Some of these are the difference between the wind velocity and the phase velocities of the various wavelengths present in the wave field, the time and fetch over which the wind has acted on these waves, and the wind's history (i.e., has it changed speed or direction?). In light of this, we kept our first attempts at including effects of wave motion on the velocity field fairly simple. However, even a very simple model of the wind and wave fields lets us qualitatively examine several aspects of the droplets' motion and concentration over a moving surface.

In a Lagrangian sense, the wave effects are modelled by describing the velocity field as

$$u(x, z, t) = \overline{U}(z) + U_w(x, z, t) + u'(x, z, t), \tag{51}$$

$$w(x, z, t) = \overline{W}(z) + W_w(x, z, t) + w'(x, z, t). \tag{52}$$

Here, the overbar denotes the horizontally averaged mean velocity, the prime terms are fluctuations resulting from turbulence, and the subscript w denotes wave-induced velocities. An obvious difficulty in using Equations (51) and (52) involves defining $\overline{U}(z)$ when z is near the moving surface (i.e., when z is sometimes under water). We handle this problem by defining a new coordinate for the vertical axis, $\zeta = z - \eta \cdot \exp(-k\zeta)$ (e.g., Taylor, 1977), where k is the principal wavenumber of the undulating surface, and η is the instantaneous wave height. In this expression, when $\zeta = 0$, $z = \eta$; and as ζ goes to infinity, $z = \zeta$.

The mean and wave-induced horizontal velocities can then be combined by using ζ in a logarithmic profile,

$$U(\zeta) = U_c + U_{w0}\mathrm{e}^{-m\zeta} + \frac{u_*}{\kappa} \ln\left(\frac{\zeta + \zeta_0}{\zeta_0}\right), \tag{53}$$

where

$$U_{w0} = \kappa\eta C_s, \tag{54}$$

ζ_0 is the roughness length, C_s is the phase velocity of the wave, u_* is the friction velocity and, again, κ is von Kármán's constant. The expression for the surface velocity is found by assuming that the irrotational flow induced by the wave motion is added to the surface current, u_s, caused by the wind stress. The exponential has been added to the surface velocity term to allow it to damp out with height; m is on the order of k. For the analysis, we used a Stokes wave,

$$\eta(x, t) = -A\cos(kx - \omega t) + \tfrac{1}{2}A^2 k\cos[2(kx - \omega t)], \tag{55}$$

where ω is the wave frequency, and $2A = H_w$ is the wave height.

For the time being, we assume that the droplet statistics are the same whether the droplets are within or well above the wave-affected field. (This assumption is a main point for future investigation.) This allows us to consider the velocity components induced by the wave and turbulent fields separately. Equation (48) then determines the droplet's velocity induced by the turbulence so that the droplet's motion in the new coordinate system can be written

$$u_d^T(x, \zeta, t) = U(x, \zeta, t), \tag{56}$$

$$w_d^T(x, \zeta, t) = W_w(x, \zeta, t) + W^d(x, \zeta, t), \tag{57}$$

where the superscript T denotes the total velocity, and the contributions of the horizontal fluctuations caused by turbulence are ignored, for simplicity. These velocities are then used with

$$z(t + \Delta t) = z(t) + w_d^T(t)\Delta t, \tag{58}$$

$$x(t + \Delta t) = x(t) + u_d^T[z(t)]\Delta t, \tag{59}$$

to produce droplet trajectories (e.g., Figure 12). The height ζ_0 is used as a lower limit below which the droplets are 'absorbed' by the water surface.

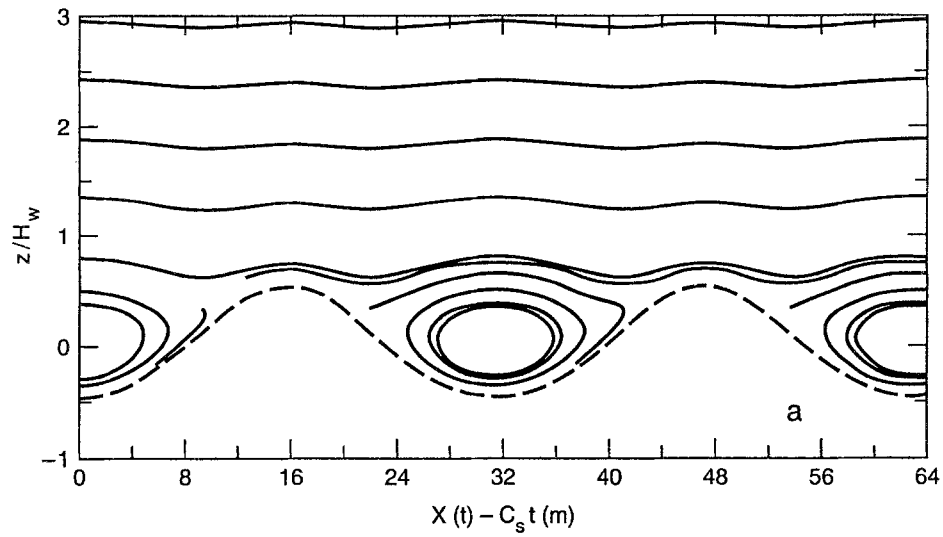

Fig. 12a.

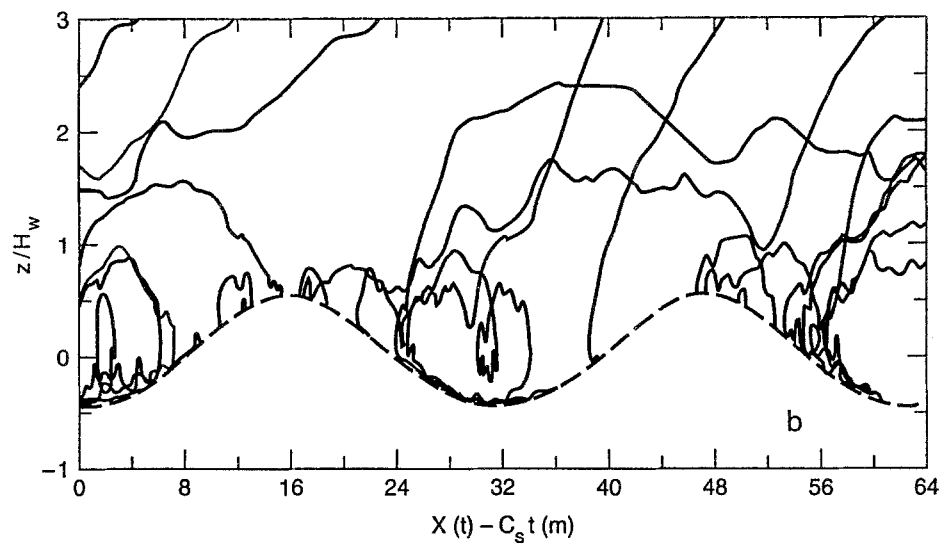

Fig. 12. Simulated conditions over a fully developed wave field. The wave amplitude, $A(= H_w/2)$ in Equation (55), is 0.785 m; the 10-m wind speed is 10 m/s; the phase speed is 7 m/s; the wavelength is 31.4 m; and, in the model, $m = 4$ k. Panel (a) shows the streamlines of the mean flow. Panel (b) shows some trajectories for nonevaporating droplets of radius 18.5 μm when the droplets are ejected along the entire wave at evenly spaced intervals.

4.3.4. Lagrangian Model Results

Figure 12 shows a case in which we selected the parameters to simulate conditions over fully developed waves. This figure displays several features that have been observed in both laboratory and oceanic studies. There is evidence of a regressive

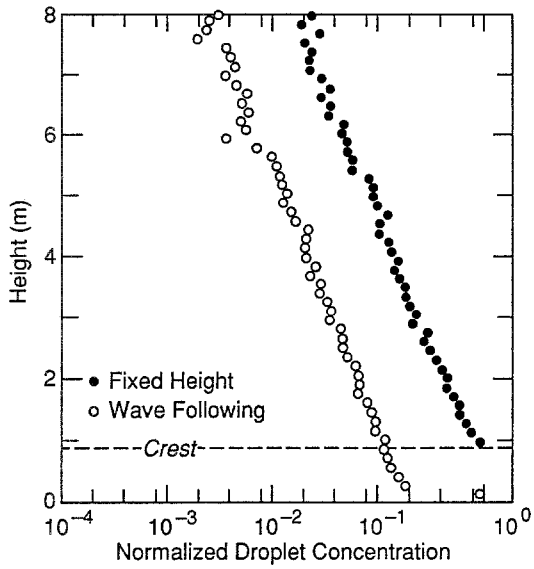

Fig. 13. Droplet concentration profiles for the conditions shown in Figure 12. The concentrations are normalized by the maximum value found at the first height.

flow very near the surface and a rotor in the trough. The figure, however, also shows an obvious oversimplification of the flow field, since the symmetry shown is not found in the laboratory measurements of Hsu *et al.* (1981) or in more complicated numerical models (e.g., Gent and Taylor, 1976).

To examine the effects that the wave-induced velocities have on the droplet concentration profiles was our principal reason for attempting this simulation. Therefore, the next step is to measure these profiles by moving an imaginary probe, either wave-riding or at fixed z, through the trajectories given in Figure 12. The model handles droplet ejection by treating the droplets as though they were elevated sources, releasing each droplet at its respective ejection height. Using the above set of equations, the model then transports the droplet along until it either falls below ζ_0 or passes the probe. If the latter occurs, its vertical position is determined above both the instantaneous and mean sea surfaces, and a count is added to these height bins (bins of 15 cm width). This process is repeated for as long as it takes to get a steady-state droplet concentration profile.

Figure 13 shows the results. Our model produced no maximum in the droplet concentration profile above the mean sea surface. This suggests that the rotor mechanism described by de Leeuw (1986b, 1987) is not responsible for the observed maximum, although this finding is far from conclusive because of the symmetry of the flow field and some of the model assumptions.

This does not mean, however, that the wave-induced velocity field has no effect on the profiles. Figure 14 shows the ratio of droplet number concentrations computed when waves are present (N_{wave}) to the concentrations computed over a

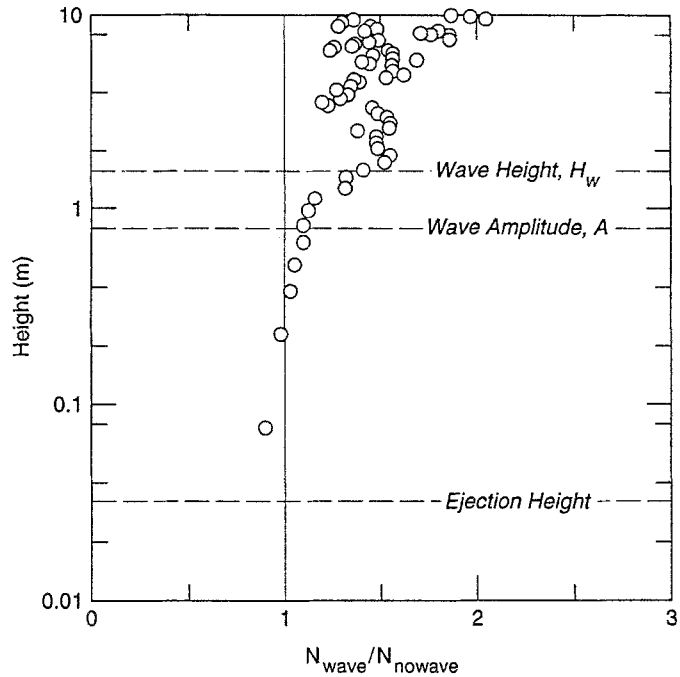

Fig. 14. Ratios of computed droplet concentration profiles with (N_{wave}) and without (N_{nowave}) waves in a coordinate system following the waves. Conditions are as in Figure 12. For droplets of 18.5 μm radius, the ejection height is about 3.2 cm (Blanchard and Woodcock, 1957).

flat ocean (N_{nowave}) – i.e, with no waves – under otherwise identical conditions. The figure shows that, in a coordinate system allowed to follow the surface, the same number of droplets exists between the ejection height and the wave amplitude for both cases. Above a height of one wave amplitude, however, we find more droplets when waves are present. In fact, at one wave height above the surface, N_{wave}/N_{nowave} becomes basically constant at 1.5 – there are 50% more droplets here when waves are present than when they are not.

Since we modelled a single-component wave, its amplitude A (see Equation (55)) corresponds to the significant-wave amplitude $A_{1/3}$. Thus, this modelling substantiates our choice of $A_{1/3}$ as the appropriate droplet length scale in (16), especially for bubble-derived droplets. (There was little question that $A_{1/3}$ was the appropriate length scale for spume droplets, since these originate near a height of $A_{1/3}$.)

The droplets depicted in Figure 14 are in a nonevaporating environment. But since the figure does demonstrate how the wave field affects the dynamics of the near-surface flow and, consequently, the dispersion of spray droplets, we can still infer from it that the top of the DEL must be at least one significant-wave height above mean sea level. In other words, we conclude from Figure 14 that

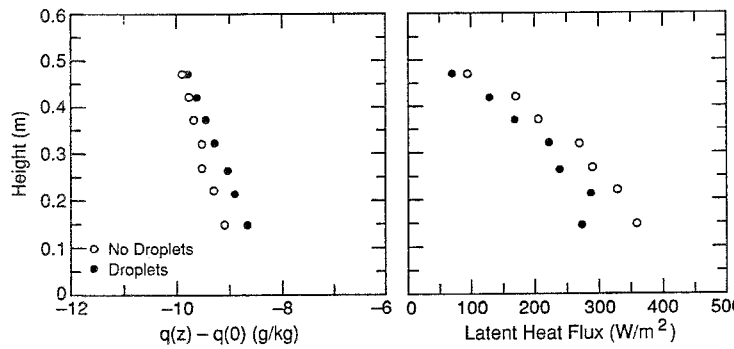

Fig. 15. Vertical profiles of specific humidity and latent heat flux, with and without spray droplets present, measured by Mestayer *et al.* (1990) during the CLUSE program. During these runs, the nominal wind speed was 7.6 m/s, and the relative humidity was 72%.

$Z2$ must be greater than $2A_{1/3}$. Thus, from Equation (11), for the high winds in HEXMAX (15–18 m/s), $Z2 > 7$–10 m.

Finally, this modelling suggests that an additional layer should be added to mixed-layer models (e.g., Fairall and Larsen, 1984) to account for wave effects.

4.4. Experimental results

Data to support our modelling were obtained during the CLUSE campaign, which devoted part of the experiment to measuring vertical flux profiles. Figure 15 shows profiles of specific humidity and latent heat flux in the presence and absence of spray droplets. (Aeration devices in the water created the droplets.) Based on droplet concentration profiles collected separately, we know that, where these measurements were made 30 m downwind of the tunnel entrance, the DEL essentially filled the 0.75-m boundary layer. In other words, these measurements were all made below $Z2$ (e.g., Figure 4). Thus, though they support the hypothesis that the evaporating droplets moisten the DEL and reduce the moisture flux from the surface, they cannot show whether or not this moisture loading leads to an eventual increase in the flux above the DEL.

The numerical models predict and these experiments document the feedbacks between spray droplets and the vertical profiles of temperature and humidity. If the heuristic ideas described in Section 4.2 or the parameterizations that we shall present in Section 5 are to be useful in future numerical models, the models must somehow account for these feedbacks.

The experiments also suggest that bulk parameterizations for sensible and latent heat fluxes could depend on the measurement height. For example, at a given wind speed, we would expect the vapor flux measured directly within the DEL to be lower than the flux measured above, while the measured specific humidity would be higher (Figures 4, 6, 9, and 10).

In summary, it appears that a complete explanation for the shape of the droplet profile, the feedbacks between the droplets and the temperature and humidity profiles, and the contribution of spume production to the heat budget will require more realistic simulations of the flow field over ocean waves than the models described above could provide. One recent study has attempted to couple the Lagrangian trajectory model described above with a two-equation turbulence model (Edson *et al.*, 1990). With this model, we hope to examine the roles played by both the turbulent flow field over waves and the spatially inhomogeneous source function in determining the droplet concentration profiles.

5. Estimates of the Spray Heat and Evaporative Fluxes

5.1. The simple analytical model

With a model for the spray generation function and with values of the microphysical and dynamic droplet time scales discussed in Section 3, we can estimate how much sea spray contributes to the air-sea fluxes of sensible and latent heat (Andreas, 1992).

Equation (14) suggests that a spray droplet returns to the sea surface with a temperature of

$$T(\tau_f) = T_{eq} + (T_w - T_{eq})\exp(-\tau_f/\tau_T). \tag{60}$$

Therefore, the rate at which all spray droplets with initial radius r_0 exchange sensible heat with the air is

$$Q_S(r_0) = \rho_s c_{ps}(T_w - T_{eq})[1 - \exp(-\tau_f/\tau_T)]\left(\frac{4}{3}\pi r_0^3 \frac{\mathrm{d}F_M}{\mathrm{d}r_0}\right). \tag{61}$$

Here, ρ_s is the density of the surface sea water, c_{ps} is the specific heat of sea water, and $\mathrm{d}F_M/\mathrm{d}r_0$ is the spray generation function based on Miller (1987) and Wu *et al.* (1984). Notice that $(4\pi r_0^3/3)(\mathrm{d}F_M/\mathrm{d}r_0)$ is the volume flux of spray droplets with initial radius r_0.

Similarly, Equation (15) shows that when $\tau_f \leq \tau_r$, a spray droplet has a radius of

$$r(\tau_f) = r_{eq} + (r_0 - r_{eq})\exp(-\tau_f/\tau_r), \tag{62}$$

when it falls back into the sea. The rate at which droplets of initial radius r_0 exchange latent heat with the air is, therefore,

$$Q_L(r_0) = -\rho_s L_v \left\{1 - \left(\frac{r(\tau_f)}{r_0}\right)^3\right\}\left(\frac{4}{3}\pi r_0^3 \frac{\mathrm{d}F_M}{\mathrm{d}r_0}\right), \quad \text{for } \tau_f \leq \tau_r. \tag{63}$$

Since our sign convention is that a positive flux adds heat to the air, the negative sign in front of Equation (63) indicates that evaporating spray droplets extract

heat from the air. That is, as we explained earlier, evaporating droplets cool the DEL.

If the relative humidity is 95% or less, at least two-thirds of the potential moisture loss has already occurred by the time droplets for which $\tau_f > \tau_r$ fall back into the sea. Thus, to estimate the latent heat extracted by these droplets, we simply assume that $\tau_f \gg \tau_r$; in effect, we assume that their mass exchange is complete. The rate at which these small droplets exchange latent heat is, thus, approximately

$$Q_L(r_0) \simeq -\rho_s L_v \left[1 - \left(\frac{r_{eq}}{r_0}\right)^3\right] \left(\frac{4}{3}\pi r_0^3 \frac{\mathrm{d}F_M}{\mathrm{d}r_0}\right), \quad \text{for } \tau_f > \tau_r. \tag{64}$$

5.2. Spray heat fluxes

With values of τ_T, τ_r, τ_f, T_{eq}, and r_{eq} (Andreas, 1989, 1990, 1992) we can now estimate spray heat flux contributions from Equations (61), (63), and (64). Figure 16 shows one such set of computations; Andreas (1992) showed several others.

By integrating under each curve in Figure 16, we can find the total spray contribution to the air-sea sensible ($\overline{Q}_S$) and latent ($\overline{Q}_L$) heat fluxes. For the indicated 10-m wind speeds, 5, 10, and 20 m/s, $\overline{Q}_S$ is 0.21, 0.78, and 15 W/m^2; and $\overline{Q}_L$ is -0.56, -3.9, and -150 W/m^2. Because of the uncertainty in the spray generation function, uncertainty in these computations is $\pm 50\%$. We can compute the corresponding interfacial (or turbulent) sensible (H_s) and latent (H_L) heat fluxes by the bulk-aerodynamic method with more certainty, say $\pm 10\%$ (Andreas, 1992). For winds of 5, 10, and 20 m/s, H_s is 13, 24, and 46 W/m^2; and H_L is 74, 140, and 260 W/m^2. Thus, for these ambient conditions, the spray fluxes contribute no more than 10% to the total air-sea heat fluxes for wind speeds up to about 15 m/s. (This 10% limit is the commonly ascribed uncertainty in *in-situ* measurements of the air-sea heat fluxes.)

Consequently, even in moderate winds, it may be difficult to separate the spray heat fluxes from the noise. At wind speeds above 15 m/s, however, both the spray sensible and latent heat fluxes become significant for these ambient conditions because the spray production increases as, roughly, the third power of the wind speed, while the turbulent fluxes increase only linearly with wind speed (e.g., Andreas, 1992).

This model result is quite compatible with the HEXMAX data, though the environment modeled in Figure 16 differs somewhat from HEXMAX conditions. A primary result from HEXMAX was that the bulk transfer coefficient for water vapor, C_E, did not increase with wind speed by more than 15–20% for 10-m wind speeds up to 18 m/s (Katsaros and DeCosmo, 1993; DeCosmo *et al.*, 1994). In other words, during HEXMAX, evaporating spray droplets contributed no more than 15–20% to the net air-sea vapor flux for winds up to 18 m/s. Andreas (1994b) ran his model for typical HEXMAX conditions and, thereby, demonstrated that it agreed with the HEXMAX data. For an air temperature of 13°C,

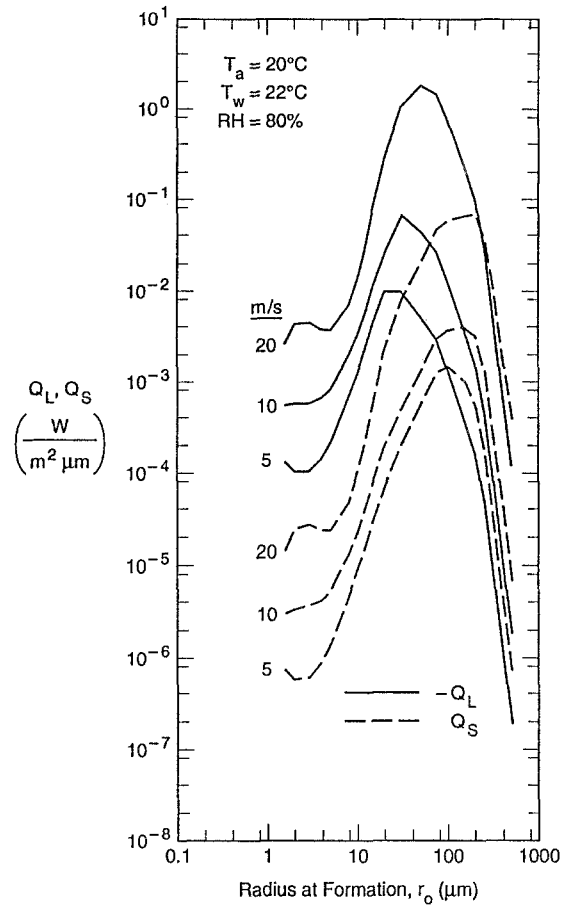

Fig. 16. The radius-specific spray sensible and latent heat fluxes within the droplet evaporation layer, Q_S and Q_L, as functions of the 10-m wind speed. Notice that Q_L is negative. Calculations are based on Miller's (1987) spray generation function, with the large-droplet extension based on Wu *et al.* (1984) (see Figure 3). Ambient conditions are T_a = 20°C, T_w = 22°C, RH = 80%, S = 34‰, and P = 1000 hPa.

the spray fluxes would have less than a 15% effect on the net fluxes for winds up to 16 m/s. As the wind gets higher than the 18-m/s maximum observed during HEXMAX, however, the modeled spray fluxes become comparable to the interfacial fluxes.

Besides letting us estimate the spray fluxes in the DEL, Figure 16 makes several other interesting points. The latent heat contributed by the smallest droplets is much larger than the sensible heat that these contribute. These small droplets, which have time to reach both thermal and moisture equilibrium (see Figure 2), simply carry much more latent than sensible heat. And this conclusion is independent of the spray generation function we use. But for the ambient conditions depicted in Figure 16, a crossover occurs as droplet radius increases. At a

radius of 100–200 μm, depending on wind speed, the sensible heat contribution becomes larger than the latent heat contribution. Andreas (1992), in fact, showed cases for which $\overline{Q}_S$ could exceed $\overline{Q}_L$ because of this crossover. Figure 2 explains this effect. Droplets in this size range fall back into the sea before exchanging significant latent heat but have ample time to participate fully in the sensible heat exchange. Hence, although they carry much less sensible than latent heat, because of the rapidity of the sensible heat transfer, droplets in this size range are important components in the air-sea transfer of sensible heat. As we explained in the last section, our numerical models currently ignore this sensible heat.

The Q_L peaks in Figure 16 move from $r_0 = 20$ μm to $r_0 = 50$ μm as wind speed increases. Similarly, the Q_S peaks move from 100 to 200 μm with increasing wind speed. Not only are more droplets produced in higher winds, but the droplets have longer to interact with their environment. Jet droplets may contribute to the Q_L peaks, but spume droplets must dominate the Q_S peaks. Figure 16, thus, establishes the importance of spume droplets in enhancing air-sea heat exchange and focuses attention on the need for corroborating or revising the spume production implied in the model based on Miller (1987) and Wu *et al.* (1984).

The locations of the Q_L peaks in Figure 16 agree well with Rouault and Larsen's (1990) model results, Figure 8, although their model did not treat spume explicitly and injected all droplets into the boundary layer at the ejection height. We conclude from the agreement between these two approaches that droplets in this size range are swept up and easily transported by the turbulence (also, see Figures 2, 11, and 12b). Therefore, for estimating the total heat and moisture that these droplets exchange, their height of origin is largely immaterial – though this height will likely affect the details of the temperature and water vapor profiles within the DEL.

We have emphasized throughout that sea spray produces a multi-layer system near the sea surface. The fluxes predicted here, $\overline{Q}_S$ and $\overline{Q}_L$, would be available within the DEL – that is, below Z2 (see Figures 4–7). But because of all the feedbacks within this layer, it is probable that not all of these fluxes rise above $Z2$ and, thereby, become available to the entire marine boundary layer.

Fairall *et al.* (1994) assumed that only a fraction of $\overline{Q}_S$ and $\overline{Q}_L$ rises above the DEL and, thus, used simple linear relationships to model the feedbacks within the DEL. In their simulation of a hurricane, Fairall *et al.* set the lower boundary conditions above the DEL such that the heat fluxes are

$$H_s(z > Z2) = H_s + \alpha\overline{Q}_S - \beta\overline{Q}_L, \tag{65}$$

$$H_L(z > Z2) = H_L + \beta\overline{Q}_L. \tag{66}$$

Here, H_s and H_L are fluxes determined using the standard bulk-aerodynamic formulas, $H_s(z > Z2)$ and $H_L(z > Z2)$ are the net fluxes at the top of the DEL, and α and β parameterize, respectively, what fractions the spray sensible

and latent heat fluxes contribute to the fluxes above the DEL. Consequently, the fluxes within the DEL are

$$H_s(z < Z2) = H_s - (1 - \alpha)\overline{Q}_S + (1 - \beta)\overline{Q}_L, \tag{67}$$

$$H_L(z < Z2) = H_L - (1 - \beta)\overline{Q}_L. \tag{68}$$

That is, their model has a two-layer structure similar to Figures 4 and 5 but without the smooth transition across $Z2$. Fairall *et al.* hypothesized that $\alpha = \beta = 0.5$. In other words, half of the spray heat fluxes within the DEL escapes out the top of this layer.

Equations (65) and (66) reiterate how difficult it will be to define effective bulk transfer coefficients for latent (C_E) and sensible (C_H) heat when spray is present. The turbulent fluxes H_s and H_L increase linearly with the wind speed, while $\overline{Q}_S$ and $\overline{Q}_L$ increase roughly as the cube of the wind speed. The sea-air difference in temperature drives H_s and $\overline{Q}_S$, and the sea-air difference in humidity drives H_L. But the air temperature alone and the relative humidity of the air determine the magnitude of $\overline{Q}_L$. Thus, for any given wind speed, sea-air temperature difference, and sea-air humidity difference, C_H and C_E will have ranges of values that depend on the air temperature and relative humidity (Andreas, 1994b). In summary, because of the large uncertainty in the spray generation function for wind speeds below 20 m/s; because we know little about that function for winds above 20 m/s, where spray effects probably dominate; and because of the uncertainty remaining in the feedback parameters α and β; we are still not quite ready to estimate C_H and C_E in conditions where spray is important.

5.3. Spray evaporative flux

Figure 17 compares the turbulent or interfacial evaporative flux (H_L/L_V) with the spray evaporative flux ($-\overline{Q}_L/L_v$) predicted by the model described in Section 5.1. The middle line in the plot is for the same conditions depicted in Figure 16. The right line is for conditions in the warm surface pool in the western, equatorial Pacific (the TOGA-COARE region). The left line models high-latitude conditions. Notice, the spray evaporative fluxes here are positive: Although evaporating spray extracts latent heat from the air (a negative flux), it adds moisture (a positive flux).

Again, these are the evaporative fluxes within the DEL. According to Fairall *et al.* (1994), about half of these fluxes would be available above the DEL. Also, as noted above, uncertainties in the spray fluxes in the figure are $\pm 50\%$.

Figure 17 demonstrates how strongly the spray flux depends on wind speed. For the three cases depicted, the turbulent evaporative fluxes increase by a factor of about four as the wind speed increases from 5 to 20 m/s. The spray evaporative fluxes, on the other hand, increase by more than two orders of magnitude over the same range in each case. For the two cases with large turbulent flux, the

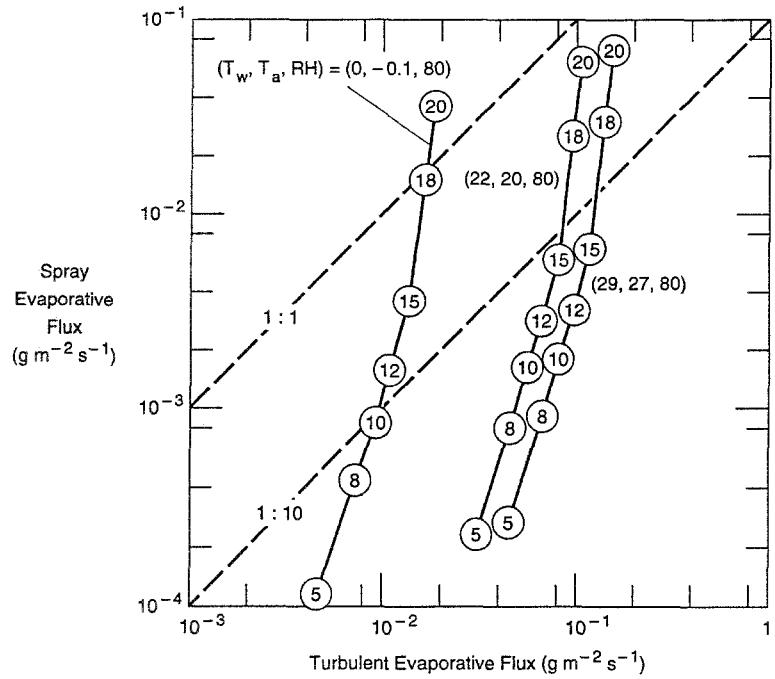

Fig. 17. Model calculations of the spray evaporative flux in the droplet evaporation layer ($-\overline{Q}_L/L_v$) versus bulk-aerodynamic estimates of the turbulent or interfacial evaporative flux (H_L/L_v) for three sets of ambient conditions. T_w and T_a are the water temperature and the air temperature (both in deg. C.); RH is the relative humidity (in percent); and P =1000 hPa. The numbers in circles give the 10-m wind speed in m/s. The diagonal lines show where the two fluxes are equal and where the spray flux is 10% of the turbulent flux.

wind speed must be above 15 m/s before the spray flux is 10% of the turbulent flux. But by 20 m/s, the spray flux is roughly 60% of the turbulent flux. In the case with relatively low turbulent flux (the high-latitude case), the spray flux is 10% of the turbulent flux when the wind speed is 10 m/s and is greater than the turbulent flux when the wind speed exceeds roughly 18 m/s. Once again, we see the need for studying spray generation in winds over 20 m/s.

6. Discussion and Conclusions

The sea spray generation function derived from Miller (1987), with a large-droplet extension based on Wu *et al.* (1984) (Figure 3), encompasses the entire range of relevant droplet sizes and is, thus, the best such function currently available. Though, admittedly, its large-droplet predictions are based on uncertain extrapolations, it predicts a spray volume flux that peaks in the spume region. In turn, our modelling has shown that spume droplets – namely, those with

radii between 10 and 300 μm – contribute most to the spray fluxes of heat and moisture.

Our modelling has also identified some of the processes important in sea spray dynamics and thermodynamics. Intuition, models, and observations all establish that surface waves are important in mixing the spray droplets upward; thus, the near-surface spray distribution scales with a wave-height parameter such as $A_{1/3}$. The region near the sea surface actually consists of several layers because of spray processes. Within a droplet evaporation layer that, again, scales with the wave amplitude, the evaporating spray moistens and cools the air. This cooling is evidence that the spray extracts sensible heat from the air in order to evaporate. Because of the elevated sources and sinks of heat within this layer, the vertical fluxes of heat and moisture are not constants with height, as they are in a typical atmospheric surface layer. Consequently, bulk parameterizations of the heat and moisture fluxes in the presence of spray may be height dependent.

The droplet time scales described in Section 3 and the analytical model in Section 5 suggest under what conditions the spray fluxes will be largest. Wind speed is the dominant factor since spray production increases, roughly, as the third power of the wind speed. Because droplet temperature determines the rate at which spray droplets evaporate, higher air temperatures foster larger spray moisture and latent heat fluxes. The actual sea-surface temperature is immaterial in spray latent heat transfer. As a result, parameterizing vapor exchange in terms of a simple bulk transfer coefficient may not adequately represent the processes active in a spray environment (Ling, 1993; Andreas, 1994b). In contrast, the sea-air temperature difference drives the spray sensible heat transfer – as well as the turbulent (or interfacial) sensible heat transfer. Thus, this spray flux will be largest where the sea-air temperature difference is largest – in high latitudes, for example.

Cess and Potter (1988) and Mitchell (1989), among others, have shown that general circulation models (GCMs) are sensitive to perturbations in the Earth's surface heat budget of only a few W m^{-2}. Our modelling shows that winds of 10 m/s can produce spray fluxes with this magnitude; in storm winds, the spray fluxes can conceivably have magnitudes that exceed those of the turbulent fluxes. The fact that no GCM yet includes a parameterization for the spray heat and moisture fluxes is understandable, given past uncertainty in the magnitudes of these fluxes. But with recent progress in understanding spray processes, the time is ripe for GCMs to begin including spray effects in oceanic heat and moisture budgets.

The growing consensus in the spray community is that understanding how spray droplets transfer heat and moisture between the ocean and atmosphere in high winds is crucial (Bortkovskii, 1973, 1987; Borisenkov, 1974; Wu, 1974; Stramska, 1987; Rouault and Larsen, 1990; Fairall *et al.*, 1994). For this reason, spray research is becoming focused on severe weather such as tropical storms and hurricanes (e.g., Fairall *et al.*, 1994). But because revolutionary droplet-

measuring technology will be needed before researchers can venture into these conditions, this research has turned to numerical modelling, where improving the modelling of spume droplets is a priority. Still, making model improvements will require continued measurements for validating the models. With the knowledge gained from past experiments and models, we can now design experiments to examine the remaining questions.

A primary requirement for future experiments will be to measure the Reynolds fluxes of sensible and latent heat at several levels within the DEL as well as above it. Such profile measurements are essential for investigating the local ignorance hypothesis depicted in Figures 4–7 and, thus, for evaluating the feedbacks and the feedback parameters α and β in (65)–(68). Because the HEXOS program developed the technology for measuring eddy fluxes in a spray environment (Fairall *et al.*, 1990b; Edson *et al.*, 1991; DeCosmo, 1991; Katsaros *et al.*, 1994; DeCosmo *et al.*, 1994) – where sea salt and sea water droplets have plagued previous investigators – there is now no reason not to plan such measurements.

Second, future experiments must focus on spume production. Although modelling and analyses point to spume droplets as the primary agents for exchanging spray heat and moisture, we still know little about the mechanism and rate of spume generation. There simply have been few *in situ* observations of how spume forms. Future experiments could make good use of recent developments in video technology (e.g., Itagaki and Ryerson, 1990; Ryerson and Longo, 1992) to study spume production.

In closing, we seem to have the conceptual and numerical tools for taking the next big step in understanding how and when sea spray affects the air-sea fluxes of heat and moisture. Good oceanic measurements will make this step easier.

Acknowledgements

We offer special thanks to G. de Leeuw, C. W. Fairall, A. W. Hogan, S. E. Larsen, P. G. Mestayer, and M. H. Smith for sharing their insights on various aspects of this problem. Lutz Hasse, on behalf of the Working Group A, Boundary-Layer Dynamics and Air-Sea Interaction, of the International Commission on Dynamic Meteorology, originally approached us about the need for writing this review. We acknowledge Working Group A's role in getting this project started and thank them for their encouragement. ELA and ECM thank the Office of Naval Research for supporting this work through contracts N00014-92-MP-22014, N00014-93-MP-22033, and N00014-94-MP-35008 and through grants N00014-87-K-0185 and N00014-91-J-1444, respectively. JBE and MPR acknowledge the support of the National Science Foundation via grants OCE-9115227 and INT-8907676. This is HEXOS Contribution 45.

References

Andreas, E. L.: 1989, 'Thermal and Size Evolution of Sea Spray Droplets', CRREL Rept. 89-11, U.S. Army Cold Regions Research and Engineering Laboratory, Hanover, N.H., 37 pp. [NTIS: AD A210484].

Andreas, E. L.: 1990, 'Time Constants for the Evolution of Sea Spray Droplets', *Tellus* **42B**, 481–497.

Andreas, E. L.: 1992, 'Sea Spray and the Turbulent Air-Sea Heat Fluxes', *J. Geophys. Res.* **97**, 11,429–11,441.

Andreas, E. L.: 1994a, 'Comments on "On the Contribution of Spray Droplets to Evaporation" by Lutz Hasse', *Boundary-Layer Meteorol.* **68**, 207–214.

Andreas, E. L.: 1994b, 'Reply', *J. Geophys. Res.* **99**, in press.

Batchelor, G. K.: 1970, *An Introduction to Fluid Dynamics*, Cambridge University Press, 615 pp.

Blanchard, D. C.: 1963, 'The Electrification of the Atmosphere by Particles from Bubbles in the Sea', in M. Sears (ed.), *Progress in Oceanography*, Vol. 1, MacMillan, New York, pp. 71–202.

Blanchard, D. C.: 1983, 'The Production, Distribution, and Bacterial Enrichment of the Sea-Salt Aerosol', in P. S. Liss and W. G. N. Slinn (eds.), *Air-Sea Exchange of Gases and Particles*, D. Reidel, Dordrecht, pp. 407–454.

Blanchard, D. C. and Syzdek, L. D.: 1988, 'Film Drop Production as a Function of Bubble Size', *J. Geophys. Res.* **93**, 3649–3654.

Blanchard, D C. and Syzdek, L. D.: 1990, 'Reply', *J. Geophys. Res.* **95**, 7393.

Blanchard, D. C. and Woodcock, A. H.: 1957, 'Bubble Formation and Modification in the Sea and its Meteorological Significance', *Tellus* **9**, 145–158.

Blanchard, D. C. and Woodcock, A. H.: 1980, 'The Production, Concentration, and Vertical Distribution of the Sea-Salt Aerosol', *Ann. N.Y. Acad. Sci.* **338**, 330–347.

Borisenkov, E. P.: 1974, 'Some Mechanisms of Atmosphere-Ocean Interaction under Stormy Weather Conditions', *Problems Arctic Antarct.* **43–44**, 73–83.

Bortkovskii, R. S.: 1973, 'On the Mechanism of Interaction between the Ocean and the Atmosphere during a Storm', *Fluid Mech.-Sov. Res.* **2**, 87–94.

Bortkovskii, R. S.: 1983, *Heat and Moisture Exchange between Atmosphere and Ocean under Storm Conditions* (in Russian), Hydrometeorological Publishing House, Leningrad, 160 pp.

Bortkovskii, R. S.: 1987, *Air-Sea Exchange of Heat and Moisture during Storms*, D. Reidel, Dordrecht, 194 pp.

Burk, S. D.: 1984, 'The Generation, Turbulent Transfer and Deposition of the Sea-Salt Aerosol', *J. Atmos. Sci.* **41**, 3040–3051.

Cess, R. D. and Potter, G. L.: 1988, 'A Methodology for Understanding and Intercomparing Atmospheric Climate Feedback Processes in General Circulation Models', *J. Geophys. Res.* **93**, 8305–8314.

Charnock, H.: 1955, 'Wind Stress on Water: An Hypothesis', *Quart. J. Roy. Meteorol. Soc.* **81**, 639.

Cipriano, R. J. and Blanchard, D. C.: 1981, 'Bubble and Aerosol Spectra Produced by a Laboratory "Breaking Wave" ', *J. Geophys. Res.* **86**, 8085–8092 .

Davidson, K. L. and Fairall, C. W.: 1986, 'Optical Properties of the Marine Atmospheric Boundary Layer: Aerosol Profiles', in *Ocean Optics VII, Proc. SPIE* **637**, Society of Photo-Optical Instrumentation Engineers, Bellingham, Wash., pp. 18–24.

DeCosmo, J.: 1991, 'Air-Sea Exchange of Momentum, Heat and Water Vapor over Whitecap Sea States', Ph.D. Thesis, Department of Atmospheric Sciences, University of Washington, Seattle, 212 pp.

DeCosmo, J., Katsaros, K. B., Smith, S. D., Anderson, R. J., Oost, W. A., Bumke, K. and Grant, A. L. M.: 1994, 'Air-Sea Exchange of Sensible Heat and Water Vapor over Whitecap Sea States', *J. Geophys. Res.*, submitted.

de Leeuw, G.: 1986a, 'Size Distribution of Giant Aerosol Particles Close above Sea Level', *J. Aerosol Sci.* **17**, 293–296.

de Leeuw, G.: 1986b, 'Vertical Profiles of Giant Particles Close above the Sea Surface', *Tellus* **38B**, 51–61.

de Leeuw, G.: 1987, 'Near-Surface Particle Size Distribution Profiles over the North Sea', *J. Geophys. Res.* **92**, 14,631–14,635.

de Leeuw, G.: 1990a, 'Comment on "Vertical Distribution of Spray Droplets near the Sea Surface: Influences of Jet Drop Ejection and Surface Tearing" ', *J. Geophys. Res.* **95**, 9779–9782.

de Leeuw, G.: 1990b, 'Profiling of Aerosol Concentrations, Particle Size Distributions and Relative Humidity in the Atmospheric Surface Layer over the North Sea', *Tellus* **42B**, 342–354.

de Leeuw, G.: 1990c, 'Spray Droplet Source Function: From Laboratory to Open Sea', in P. G. Mestayer, E. C. Monahan, and P. A. Beetham (eds.), *Modelling the Fate and Influence of Marine Spray*, Whitecap Rept. 7, University of Connecticut, Marine Sciences Institute, Groton, pp. 17–28. [Available from E. C. Monahan].

Donelan, M.: 1990, 'Air-Sea Interaction', in B. Le Méhauté and D. M. Hanes (eds.), *The Sea*, Vol. 9A, Wiley-Interscience, New York, pp. 239–292.

Dufour, L. and Defay, R.: 1963, *Thermodynamics of Clouds*, Academic Press, New York, 255 pp.

Earle, M. D.: 1979, 'Practical Determinations of Design Wave Conditions', in M. D. Earle and A. Malahoff (eds.), *Ocean Wave Climate*, Plenum Press, New York, pp. 39–60.

Edson, J. B.: 1989, 'Lagrangian Model Simulation of the Turbulent Transport of Evaporating Jet Droplets', Ph.D. Thesis, Department of Meteorology, The Pennsylvania State University, University Park, 142 pp.

Edson, J. B.: 1990, 'Simulating Droplet Motion above a Moving Surface', in P. G. Mestayer, E. C. Monahan, and P. A. Beetham (eds.), *Modelling the Fate and Influence of Marine Spray*, Whitecap Rept. 7, University of Connecticut, Marine Sciences Institute, Groton, pp. 171-174. [Available from E. C. Monahan].

Edson, J. B. and Fairall, C. W.: 1994, 'Lagrangian Model Simulation of the Turbulent Transport of Evaporating Spray Droplets', *J. Geophys. Res.*, in press.

Edson, J. B., Lévi-Alvarés, S., Sini, J. F. and Mestayer, P. G.: 1990, 'GWAIHIR: A Combined Eulerian/Lagrangian Model of the Transport of Heavy Particles in Turbulent Flows', Note Interne No. H.90.03, ENSM-LMTTD, Nantes, France, 36 pp.

Edson, J. B., Fairall, C. W., Mestayer, P. G. and Larsen, S. E.: 1991, 'A Study of the Inertial-Dissipation Method for Computing Air-Sea Fluxes', *J. Geophys. Res.* **96**, 10,689–10,711.

Eriksson, E.: 1959, 'The Yearly Circulation of Chloride and Sulfur in Nature; Meteorological, Geophysical and Pedological Implications, Part I', *Tellus* **11**, 375–403.

Eriksson, E.: 1960, 'The Yearly Circulation of Chloride and Sulfur in Nature; Meteorological, Geophysical and Pedological Implications, Part II', *Tellus* **12**, 63–109.

Exton, H. J., Latham, J., Park, P. M., Perry, S. J., Smith, M. H. and Allan, R. R.: 1985, 'The Production and Dispersal of Marine Aerosol', *Quart. J. Roy. Meteorol. Soc.* **111**, 817–837.

Fairall, C. W. and Edson, J. B.: 1989, 'Modeling the Droplet Contribution to the Sea-to-Air Moisture Flux', in E. C. Monahan and M. A. Van Patten (eds.), *The Climate and Health Implications of Bubble-Mediated Sea-Air Exchange*, Connecticut Sea Grant Program, Groton, pp. 121–146.

Fairall, C. W. and Larsen, S. E.: 1984, 'Dry Deposition, Surface Production and Dynamics of Aerosols in the Marine Boundary Layer', *Atmos. Environ.* **18**, 69–77.

Fairall, C. W., Davidson, K. L. and Schacher, G. E.: 1983, 'An Analysis of the Surface Production of Sea-Salt Aerosols', *Tellus* **35B**, 31–39.

Fairall, C. W., Edson, J. B. and Miller, M. A.: 1990a, 'Heat Fluxes, Whitecaps, and Sea Spray', in G. L. Geernaert and W. J. Plant (eds.), *Surface Waves and Fluxes*, Vol. 1, Kluwer, Dordrecht, pp. 173–208.

Fairall, C. W., Edson, J. B., Larsen, S. E. and Mestayer, P. G.: 1990b, 'Inertial-Dissipation Air-Sea Flux Measurements: A Prototype System Using Realtime Spectral Computations', *J. Atmos. Oceanic Technol.* **7**, 425–453.

Fairall, C. W., Kepert, J. D. and Holland, G. J.: 1994, 'The Effect of Sea Spray on Surface Energy Transports over the Ocean', *Atmos.-Ocean System*, in press.

Fitzgerald, J. W.: 1975, 'Approximation Formulas for the Equilibrium Size of an Aerosol Particle as a Function of its Dry Size and Composition and the Ambient Relative Humidity', *J. Appl. Meteorol.* **14**, 1044–1049.

Friedlander, S. K.: 1977, *Smoke, Dust and Haze: Fundamentals of Aerosol Behavior*, John Wiley, New York, 317 pp.

Gathman, S. G.: 1982, 'A Time-Dependent Oceanic Aerosol Profile Model', NRL Rept. 8536, Naval Research Laboratory, Washington, D.C., 35 pp.

Gent, P. R. and Taylor, P. A.: 1976, 'A Numerical Model of the Air Flow above Water Waves', *J. Fluid Mech.* **77**, 105–128.

Hasse, L.: 1992, 'On the Contribution of Spray Droplets to Evaporation', *Boundary-Layer Meteorol.* **61**, 309–313.

Hasse, L.: 1994, 'Reply', *Boundary-Layer Meteorol.* **69**, 335–339.

Hokusai, K. C.: 1833, 'Fishing Boat at Choshi in Soshu', from series Chie no Umi, The Art Institute of Chicago.

Hsu, C. T., Hsu, E. Y. and Street, R. L.: 1981, 'On the Structure of Turbulent Flow over a Progressive Water Wave: Theory and Experiment in a Transformed, Wave-Following Co-ordinate System', *J. Fluid Mech.* **105**, 87–117.

Iida, N., Toba, Y. and Chaen, M.: 1992, 'A New Expression for the Production Rate of Sea Water Droplets on the Sea Surface', *J. Oceanogr.* **48**, 439–460.

Iribarne, J. V. and Godson, W. L.: 1981, *Atmospheric Thermodynamics*, 2nd edition, D. Reidel, Dordrecht, 259 pp.

Itagaki, K. and Ryerson, C. C.: 1990, 'A Universal Flying Particle Camera', 5th International Workshop on Atmospheric Icing of Structures, 29 October – 1 November 1990, Tokyo, Japanese Society of Snow and Ice, pp. B2-1-(1) to B2-1-(4).

Jacobs, W. C.: 1937, 'Preliminary Report on a Study of Atmospheric Chlorides', *Mon. Weath. Rev.* **65**, 147–151.

Junge, C. E.: 1957, 'The Vertical Distribution of Aerosols over the Ocean', in H. Weickmann and W. Smith (eds.), *Artificial Stimulation of Rain*, Pergamon Press, New York, pp. 89–96.

Katsaros, K. B. and DeCosmo, J.: 1993, 'Water Vapor Flux from the Sea at High Wind Speeds', in J. Lighthill, Z. Zhemin, G. Holland and K. Emanuel (eds.), *Tropical Cyclone Disasters*, Peking University Press, Beijing, China, pp. 386–392.

Katsaros, K. B. and de Leeuw, G.: 1994, 'Comment on "Sea Spray and the Turbulent Air-Sea Heat Fluxes," by E. L. Andreas', *J. Geophys. Res.* **99**, in press.

Katsaros, K. B., Smith, S. D. and Oost, W. A.: 1987, 'HEXOS – Humidity Exchange over the Sea, a Program for Research on Water-Vapor and Droplet Fluxes from Sea to Air at Moderate to High Wind Speeds', *Bull. Amer. Meteorol. Soc.* **68**, 466–476.

Katsaros, K. B., DeCosmo, J., Lind, R. J., Anderson, R. J., Smith, S. D., Krann, C., Oost, W., Uhlig, K., Mestayer, P. G., Larsen, S. E., Smith, M. H. and de Leeuw, G.: 1994, 'Measurements of Humidity and Temperature in the Marine Environment during the HEXOS Main Experiment', *J. Atmos. Oceanic Technol.* **11**, in press.

Kientzler, C. F., Arons, A. B., Blandhard, D. C. and Woodcock, A. H.: 1954, 'Photographic Investigation of the Projection of Droplets by Bubbles Bursting at a Water Surface', *Tellus* **6**, 1–7.

Kinsman, B.: 1965, *Wind Waves*, Prentice-Hall, Englewood Cliff, N.J., 676 pp.

Ling, S. C.: 1993, 'Effect of Breaking Waves on the Transport of Heat and Water Vapor Fluxes from the Ocean', *J. Phys. Oceanogr.* **23**, 2360–2372.

Ling, S. C. and Kao, T. W.: 1976, 'Parameterization of the Moisture and Heat Transfer Process over the Ocean under Whitecap Sea States', *J. Phys. Oceanogr.* **6**, 306–315.

Ling, S. C., Saad, A. and Kao, T. W.: 1978, 'Mechanics of Multiphase Fluxes over the Ocean', in A. Favre and K. Hasselmann (eds.), *Turbulent Fluxes through the Sea Surface, Wave Dynamics, and Prediction*, Plenum Press, New York, pp. 185–194.

Ling, S. C., Kao, T. W. and Saad, A. I.: 1980, 'Microdroplets and Transport of Moisture from Ocean', *Proc. ASCE, Engng. Mech. Div.* **106**, 1327–1339.

Meek, C. C. and Jones, B. G.: 1973, 'Studies of the Behavior of Heavy Particles in a Turbulent Fluid Flow', *J. Atmos. Sci.* **30**, 239–244.

Mestayer, P. and Lefauconnier, C.: 1988, 'Spray Droplet Generation, Transport, and Evaporation in a Wind Wave Tunnel during the Humidity Exchange over the Sea Experiments in the Simulation Tunnel', *J. Geophys. Res.* **93**, 572–586.

Mestayer, P. G., Edson, J. B., Rouault, M. P., Fairall, C. W., Larsen, S. E., de Leeuw, G., Spiel, D. E., DeCosmo, J., Katsaros, K. B., Monahan, E. C. and Schiestel, R.: 1990, 'CLUSE Simulations

of the Vapor Flux Modification by Droplet Evaporation', in P. G. Mestayer, E. C. Monahan, and P. A. Beetham (eds.), *Modelling the Fate and Influence of Marine Spray*, Whitecap Rept. 7, University of Connecticut, Marine Sciences Institute, Groton, pp. 100–105. [Available from E. C. Monahan].

Miller, M. A.: 1987, 'An Investigation of Aerosol Generation in the Marine Planetary Boundary Layer', M.S. Thesis, Department of Meteorology, The Pennsylvania State University, University Park, 142 pp.

Miller, M. A. and Fairall, C. W.: 1988, 'A New Parameterization of Spray Droplet Production by Oceanic Whitecaps', Preprint Volume, Seventh Conference on Ocean-Atmosphere Interaction, 31 January – 5 February 1988, Anaheim, Calif., American Meteorological Society, Boston, pp. 174–177.

Mitchell, J. F. B.: 1989, 'The "Greenhouse Effect" and Climate Change', *Rev. Geophys.* **27**, 115–139.

Monahan, E. C.: 1971, 'Oceanic Whitecaps', *J. Phys. Oceanogr.* **1**, 139–144.

Monahan, E. C.: 1986, 'The Ocean as a Source for Atmospheric Particles', in P. Buat-Menard (ed.), *The Role of Air-Sea Exchange in Geochemical Cycling*, D. Reidel, Dordrecht, pp. 129–163.

Monahan, E. C.: 1993, 'Occurrence and Evolution of Acoustically Relevant Sub-Surface Bubble Plumes and Their Associated, Remotely Monitorable, Surface Whitecaps', in B. R. Kerman (ed.), *Natural Physical Sources of Underwater Sound*, Kluwer, Dordrecht, pp. 503–517.

Monahan, E. C. and Lu, M.: 1990, 'Acoustically Relevant Bubble Assemblages and Their Dependence on Meteorological Parameters', *IEEE J. Oceanic Engng.* **15**, 340–349 .

Monahan, E. C. and O'Muircheartaigh, I.: 1980, 'Optimal Power-Law Description of Oceanic Whitecap Coverage Dependence on Wind Speed', *J. Phys. Oceanogr.* **10**, 2094–2099.

Monahan, E. C. and O'Muircheartaigh, I. G.: 1986, 'Whitecaps and the Passive Remote Sensing of the Ocean Surface', *Int. J. Remote Sensing* **7**, 627–642.

Monahan, E. C. and Woolf, D. K.: 1989, 'Comments on "Variations of Whitecap Coverage with Wind Stress and Water Temperature" ', *J. Phys. Oceanogr.* **19**, 706–709.

Monahan, E. C., Davidson, K. L. and Spiel, D. E.: 1982, 'Whitecap Aerosol Productivity Deduced from Simulation Tank Measurements', *J. Geophys. Res.* **87**, 8898–8904.

Monahan, E. C., Spiel, D. E. and Davidson, K. L.: 1983a, 'Model of Marine Aerosol Generation via Whitecaps and Wave Disruption', Preprint Volume, Ninth Conference on Aerospace and Aeronautical Meteorology, 6–9 June 1983, Omaha, Neb., American Meteorological Society, Boston, pp. 147–158.

Monahan, E. C., Fairall, C. W., Davidson, K. L. and Boyle, P. J.: 1983b, 'Observed Inter-Relations between 10 m Winds, Ocean Whitecaps and Marine Aerosols', *Quart. J. Roy. Meteorol. Soc.* **109**, 379–392.

Monahan, E. C., Spiel, D. E. and Davidson, K. L.: 1986, 'A Model of Marine Aerosol Generation via Whitecaps and Wave Disruption', in E. C. Monahan and G. Mac Niocaill (eds.), *Oceanic Whitecaps and Their Role in Air-Sea Exchange Processes*, D. Reidel, Dordrecht, pp. 167–174.

Montgomery, R. B.: 1940, 'Observations of Vertical Humidity Distribution above the Ocean Surface and Their Relation to Evaporation', *Papers Phys. Oceanogr. Meteorol.*, Vol. 7, No. 4, Woods Hole Oceanographic Institution, Woods Hole, Mass., 30 pp.

Mostafa, A. A. and Mongia, H. C.: 1987, 'On the Modeling of Turbulent Evaporating Sprays: Eulerian versus Lagrangian Approach', *Int. J. Heat Mass Transfer* **30**, 2583–2593.

Nieuwstadt, F. T. M.: 1984, 'The Turbulent Structure of the Stable Nocturnal Boundary Layer', *J. Atmos. Sci.* **41**, 2202–2216.

Pierson, W. J., Jr.: 1990, 'Dependence of Radar Backscatter on Environmental Parameters', in G. L. Geernaert and W. J. Plant (eds.), *Surface Waves and Fluxes*, Vol. 2, Kluwer, Dordrecht, pp. 173–220.

Preobrazhenskii, L. Yu.: 1973, 'Estimation of the Content of Spray-Drops in the Near-Water Layer of the Atmosphere', *Fluid Mech.-Sov. Res.* **2**, 95–100.

Pruppacher, H. R. and Klett, J. D.: 1978, *Microphysics of Clouds and Precipitation*, D. Reidel, Dordrecht, 714 pp.

Resch, F.: 1986, 'Oceanic Air Bubbles as Generators of Marine Aerosols', in E. C. Monahan and G. Mac Niocaill (eds.), *Oceanic Whitecaps and Their Role in Air-Sea Exchange Processes*, D. Reidel, Dordrecht, pp. 101–112.

Resch, F. and Afeti, G.: 1991, 'Film Drop Distributions from Bubbles Bursting in Seawater', *J. Geophys. Res.* **96**, 10,681–10,688.

Roll, H. U.: 1965, *Physics of the Marine Atmosphere*, Academic Press, New York, 426 pp.

Ross, D. B. and Cardone, V.: 1974, 'Observations of Oceanic Whitecaps and Their Relation to Remote Measurements of Surface Wind Speed', *J. Geophys. Res.* **79**, 444–452.

Rouault, M. P. and Larsen, S. E.: 1990, 'Spray Droplets under Turbulent Conditions', Risø-M-2845, Department of Meteorology and Wind Energy, Risø National Laboratory, Roskilde, Denmark, 60 pp.

Rouault, M. P., Mestayer, P. G. and Schiestel, R.: 1991, 'A Model of Evaporating Spray Droplet Dispersion', *J. Geophys. Res.* **96**, 7181–7200.

Ryerson, C. C. and Longo, P. D.: 1992, 'Ship Superstructure Icing: Data Collection and Instrument Performance on USCGC *Midgett* Research Cruise', CRREL Rept. 92–23, U.S. Army Cold Regions Research and Engineering Laboratory, Hanover, N.H., 133 pp. [NTIS: AD A262557].

Smith, M. H., Hill, M. K., Park, P. M. and Consterdine, I. E.: 1990, 'Aerosol Concentrations and Estimated Fluxes over the Sea', in P. G. Mestayer, E. C. Monahan, and P. A. Beetham (eds.), *Modelling the Fate and Influence of Marine Spray,* Whitecap Rept. 7, University of Connecticut, Marine Sciences Institute, Groton, pp. 40–47. [Available from E. C. Monahan].

Smith, M. H., Park, P. M. and Consterdine, I. E.: 1993, 'Marine Aerosol Concentrations and Estimated Fluxes over the Sea', *Quart. J. Roy. Meteorol. Soc.* **119**, 809–824.

Smith, S. D.: 1989, 'Water Vapor Flux at the Sea Surface', *Boundary-Layer Meteorol.* **47**, 277–293.

Smith, S. D.: 1990, 'Influence of Droplet Evaporation on HEXOS Humidity and Temperature Profiles', in P. G. Mestayer, E. C. Monahan, and P. A. Beetham (eds.), *Modelling the Fate and Influence of Marine Spray*, Whitecap Rept. 7, University of Connecticut, Marine Sciences Institute, Groton, pp. 171–174. [Available from E. C. Monahan].

Smith, S. D., Katsaros, K. B., Oost, W. A. and Mestayer, P. G.: 1990, 'Two Major Experiments in the Humidity Exchange over the Sea (HEXOS) Program', *Bull. Amer. Meteorol. Soc.* **71**, 161–172.

Smith, S. D., Anderson, R. J., Oost, W. A., Kraan, C., Maat, N., DeCosmo, J., Katsaros, K. B., Davidson, K. L., Bumke, K., Hasse, L. and Chadwick, H.: 1992, 'Sea Surface Wind Stress and Drag Coefficients: The HEXOS Results', *Boundary-Layer Meteorol.* **60**, 109–142.

Sorbjan, Z.: 1986, 'On Similarity in the Atmospheric Boundary Layer', *Boundary-Layer Meteorol.* **34**, 377–397.

Spiel, D. E.: 1992, 'Acoustical Measurements of Air Bubbles Bursting at a Water Surface: Bursting Bubbles as Helmholtz Resonators', *J. Geophys. Res.* **97**, 11,443–11,452.

Stramska, M.: 1987, 'Vertical Profiles of Sea Salt Aerosol in the Atmospheric Surface Layer: A Numerical Model', *Acta Geophys. Polonica* **35**, 87–100.

Taylor, P. A.: 1977, 'Some Numerical Solutions of Surface Boundary-Layer Flow above Gentle Topography', *Boundary-Layer Meteorol.* **11**, 439–465.

Thorpe, S. A.: 1982, 'On the Clouds of Bubbles Formed by Breaking Wind-Waves in Deep Water and Their Role in Air-Sea Gas Transfer', *Phil. Trans. Roy. Soc., London* **A304**, 155-210.

Thorpe, S. A.: 1983, 'Bubble Clouds', *Weather* **38**, 66–70.

Thorpe, S. A. and Hall, A. J.: 1983, 'The Characteristics of Breaking Waves, Bubble Clouds, and Near-Surface Currents Observed Using Side-Scan Sonar', *Continental Shelf Res.* **1**, 353–384.

Toba, Y.: 1965a, 'On the Giant Sea-Salt Particles in the Atmosphere. I. General Features of the Distribution', *Tellus* **17**, 131–145.

Toba, Y.: 1965b, 'On the Giant Sea-Salt Particles in the Atmosphere. II. Theory of the Vertical Distribution in the 10-m Layer over the Ocean', *Tellus* **17**, 365–382.

Toba, Y.: 1966, 'On the Giant Sea-Salt Particles in the Atmosphere. III. An Estimation of the Production and Distribution over the World Ocean', *Tellus* **18**, 132–145.

Wilson, B. W.: 1965, 'Numerical Prediction of Ocean Waves in the North Atlantic for December, 1959', *Deutsch. Hydrogr. Zeit.* **18**, 114–130.

Woodcock, A. H.: 1953, 'Salt Nuclei in Marine Air as a Function of Altitude and Wind Force', *J. Meteorol.* **10**, 362–371.
Woodcock, A. H.: 1972, 'Smaller Salt Particles in Oceanic Air and Bubble Behavior in the Sea', *J. Geophys. Res.* **77**, 5316–5321.
Woolf, D. K.: 1990, 'Comment on an Article by J. Wu', *Tellus* **42B**, 385–386.
Woolf, D. K., Bowyer, P. A. and Monahan, E. C.: 1987, 'Discriminating between the Film-Drops and Jet-Drops Produced by a Simulated Whitecap', *J. Geophys. Res.* **92**, 5142–5150.
Woolf, D. K., Monahan, E. C. and Spiel, D. E.: 1988, 'Quantification of the Marine Aerosol Produced by Whitecaps', Preprint Volume, *Seventh Conference on Ocean-Atmosphere Interaction*, 31 January – 5 February 1988, Anaheim, Calif., American Meteorological Society, Boston, pp. 182-185.
Wu, J.: 1973, 'Spray in the Atmospheric Surface Layer: Laboratory Study', *J. Geophys. Res.* **78**, 511–519.
Wu, J.: 1974, 'Evaporation Due to Spray', *J. Geophys. Res.* **79**, 4107–4109.
Wu, J.: 1979a, 'Oceanic Whitecaps and Sea State', *J. Phys. Oceanogr.* **9**, 1064–1068.
Wu, J.: 1979b, 'Spray in the Atmospheric Surface Layer: Review and Analysis of Laboratory and Oceanic Results', *J. Geophys. Res.* **84**, 1693–1704.
Wu, J.: 1988a, 'On Nondimensional Correlation between Roughness Length and Wind-Friction Velocity', *J. Oceanogr. Soc. Japan* **44**, 254–260.
Wu, J.: 1988b, 'Variations of Whitecap Coverage with Wind Stress and Water Temperature', *J. Phys. Oceanogr.* **18**, 1448–1453.
Wu, J.: 1989a, 'Contributions of Film and Jet Drops to Marine Aerosols Produced at the Sea Surface', *Tellus* **41B**, 469–473.
Wu, J.: 1989b, 'Reply', *J. Phys. Oceanogr.* **19**, 710–711.
Wu, J.: 1990a, 'Comment on "Film Drop Production as a Function of Bubble Size" by D. C. Blanchard and L. D. Syzdek', *J. Geophys. Res.* **95**, 7389–7391.
Wu, J.: 1990b, 'On Parameterization of Sea Spray', *J. Geophys. Res.* **95**, 18,269–18,279.
Wu, J.: 1990c, 'Reply to D. K. Woolf', *Tellus* **42B**, 387–388.
Wu, J.: 1990d, 'Vertical Distribution of Spray Droplets near the Sea Surface: Influences of Jet Drop Ejection and Surface Tearing', *J. Geophys. Res.* **95**, 9775–9778.
Wu, J.: 1992, 'Bubble Flux and Marine Aerosol Spectra under Various Wind Velocities', *J. Geophys. Res.* **97**, 2327–2333.
Wu, J.: 1993, 'Production of Spume Drops by the Wind Tearing of Wave Crests: The Search for Quantification', *J. Geophys. Res.* **98**, 18,221–18,227.
Wu, J., Murray, J. J. and Lai, R. J.: 1984, 'Production and Distributions of Sea Spray', *J. Geophys. Res.* **89**, 8163–8169.